

## Dynamic Mechanical Analysis of Magnetic Tapes at Ultra-Low Frequencies

Nicholas J. Rummel, Brian L. Weick

Mechanical Engineering Department, School of Engineering and Computer Science, University of the Pacific, Stockton, California 95211

Correspondence to: B. L. Weick (E-mail: bweick@pacific.edu)

**ABSTRACT:** A custom, ultra-low frequency, dynamic mechanical analyzer (ULDMA) has been developed to study the correlated effects of temperature and frequency on the viscoelastic behavior of magnetic tapes. It has been used to acquire data needed for the development of future magnetic tapes that require an archival life of up to 100 years. A range of elevated temperatures is used to simulate real-world storage environments, which enables the investigation of how the viscoelastic characteristics of tape samples influence the extent to which the tape deforms. The experiments and subsequent analysis examine the influence of the molecular structure on the viscoelasticity of magnetic tapes. Experiments were performed on a variety of magnetic tapes, including poly(ethylene terephthalate) (PET), poly(ethylene naphthalate) (PEN), metalized PET (M-PET), and metalized Spaltan (M-SPA). Additional experiments examined PEN and PET substrates by removing the front and back magnetic layers from the tape sample. Because of the viscoelastic behavior of the tapes, a time delay was present between the strain and stress signals, which was determined using a Fourier transform program. The elastic modulus ( $E$ ), storage modulus ( $E'$ ), loss modulus ( $E''$ ), and loss tangent ( $\tan \delta$ ) were obtained from the time delay for each of the ULDMA experiments at 25, 50, and 70°C over the frequency range of 0.0100–0.0667 Hz. Plots of these mechanical characteristics demonstrate the ability of frequency and temperature to affect trends associated with mechanical and thermal properties. Finally, some samples displayed an initial relaxation during the ULDMA experiments, which, when modeled using Maxwell's viscoelastic model, provided an insight into the relaxation characteristics of the samples. © 2012 Wiley Periodicals, Inc. *J. Appl. Polym. Sci.* 000: 000–000, 2012

**KEYWORDS:** viscoelastic properties; modulus; relaxation; polyesters; glass transition

Received 11 July 2011; accepted 13 March 2012; published online

DOI: 10.1002/app.37693

### INTRODUCTION

#### Background and Motivation

The world is generating data, specifically electronic data, at an extraordinary rate. The volume of these data continues to increase each year, and it is estimated that in the year 2011, ~ 1600 exabytes (two billion gigabytes) of information will be generated.<sup>1</sup> In 2006 alone, over \$1.79 billion dollars worth of tape drives were sold.<sup>1</sup> Advancements in technological fields serve as the primary source for this increase in data production. As of the year 2000, paper served as the primary medium for storing data, at approximately 95% of all stored data.<sup>2</sup> Recently, however, the continued development of digital storage media provides another, more efficient, manner in which data can be stored; digitally. Digital media includes compact discs, hard drives, as well as magnetic storage devices, to name a few. Although compact discs and hard drives dominate digital storage on the commercial front, magnetic tape storage is the main method used for the long-term archival storage in industry. It

has been the magnetic tape industry's goal to increase the storage capacity of magnetic tapes each year by decreasing the thickness of the magnetic films and polymeric substrates. Over the last 10 years, the capacity of the magnetic tapes has risen from 100 GB to over 1000 GB.<sup>1</sup> Additionally, the cost of magnetic storage is decreasing each year. It is estimated that by the end of 2011, the cost of a gigabyte of storage will be \$1, while the cost in 2006 was approximately \$8.<sup>1</sup> Because of the high volumetric density and data rates, as well as reliability and the low cost per gigabyte, magnetic tapes are the most practical method for storing large amounts of digital data. As the primary medium for archival storage, it is essential to improve the dynamic stability of the magnetic tapes to ensure their functionality persists for up to 100 years, as would be required for storing the medical information for the lifetime of a patient.

Advanced micro- and nanomanufacturing technologies are constantly developing improved methods for decreasing the thickness of magnetic tape substrates and decreasing the size of the

© 2012 Wiley Periodicals, Inc.

magnetic particles so that the areal density and volume of information stored in a tape reel can increase. However, as the thickness of the film decreases and the areal density increases, the dimensional stability is more susceptible to storage forces and elevated temperatures, which could lead to increased viscoelastic deformation. Reliability problems arise due to film deformation, which results in anisotropic mechanical properties. These deformations alter the dynamics between the drive head and tape, permitting the development of errors in processes associated with storing and reading data. Additionally, it is important to understand how the viscoelastic properties of polymers affect the tape-head interface. The extent to which a polymer deforms when subjected to stress depends on the viscoelastic characteristics of the polymer. The amount of deformation can affect the width of the tape sample and alter the alignment of the magnetic tape with the drive-head, which can cause a lack of tape-to-head conformity, leading to increased wear on the head.<sup>3</sup> Therefore, it is essential for tape manufacturers to understand how the material properties of magnetic tapes change as the thickness decreases, and areal density increases, to ensure that the tapes function reliably.

Multiple experimental methods have been developed and utilized over the years to measure properties and characteristics of magnetic tapes and their constitutive layers to gain a fundamental understanding of their dimensional stability. These methods include creep-compliance experiments, stress-relaxation experiments, and dynamic mechanical analysis (DMA), as well as in-cartridge creep experiments.<sup>1,2</sup> Of these methods, DMA provides the most useful connection to fundamental molecular-level behavior of the polymers used for the substrate, binder in the front coat, and back coat. In comparison, even though creep-compliance, stress-relaxation, and in-cartridge creep measurements provide relevant long-term property characteristics, it is difficult to connect these measurements to fundamental molecular behavior. Therefore, the development and utilization of a custom ultra-low frequency dynamic mechanical analyzer (ULDMA) enables fundamental molecular-level behavior to be studied at ultra-low frequency levels that approach the level of creep, at least in the limit as the frequency reaches a minimal level. In turn, the property data acquired from ULDMA can assist with the prediction of the archival life of future tapes based on the constitutive behavior of substrates, front coats, and back coats currently under development. The ability to design magnetic tapes and store them in a reel for 100+ years with the firm knowledge that the information can be read-back from the tape after that time period, is the ultimate motivation for this research.

### Magnetic Tape Properties

One of the primary methods used to increase the volumetric density of magnetic tapes involves decreasing the thickness of the magnetic tape substrate. A decreased substrate thickness allows a higher volume of magnetic tape to be stored on a reel. Another method involves increasing the areal density of tape (measured in bits per square inch), which is the product of track density and linear density. Track density refers to how tightly concentric tracks are packed, while linear density refers to how tightly bits are packed within a length of track.<sup>4</sup> As the

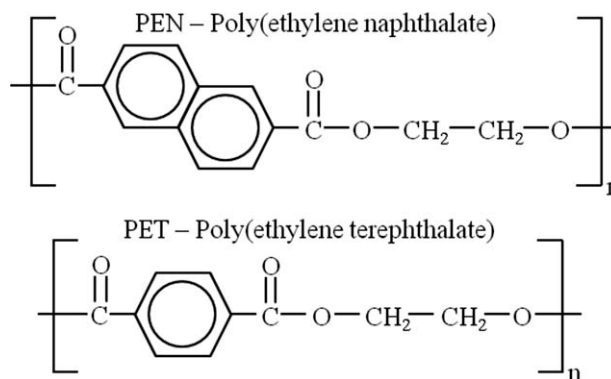


Figure 1. Chemical structures of PEN and PET.

areal density is increased, the dimensional stability of the substrates is a primary area of concern due to the fact that the substrate comprises approximately 75% of the total thickness of a magnetic tape.<sup>1</sup> The substrates must have high mechanical stability and surface smoothness to produce high areal densities. Magnetic tape manufacturers are currently researching the thermal and mechanical properties of a variety of polymers in an effort to produce an optimal substrate material. Desirable substrate properties include a high modulus of elasticity, yield strength, and tensile strength. Additionally, due to the high temperature manufacturing processes associated with magnetic film deposition, mechanical stability of the substrate is required up to 100–150°C. Low friction and high durability are also major considerations when choosing substrate materials.<sup>2</sup>

Particulate tapes and metal evaporated tapes are the two primary types of magnetic tapes; however, this article will solely focus on particulate tapes. Particulate tapes consist of several layers, specifically the front coat, substrate, and back coat. The most common materials currently employed as magnetic tape substrates are poly(ethylene naphthalate) (PEN) and poly(ethylene terephthalate) (PET). PEN and PET have nearly identical chemical structures, as shown in Figure 1, although PEN contains a naphthalene ring while PET contains a single benzene ring in each repeat unit. The ethylene glycol units of each polymer are the same, and separated identically by the rigid naphthalene ring for PEN, and benzene ring for PET, meaning they are equally flexible.<sup>5</sup> However, due to the orientation of the bonds between the ethylene glycol groups and the naphthalene ring for PEN, the molecular structure of PEN is more three-dimensional than that of the more linear PET. Because of this difference in spatial arrangement, the rotations of the PEN molecule about the naphthalene ring result in greater relative displacement of the attached ethylene glycol fragments.<sup>5</sup> This increased displacement results in a larger amount of energy dissipation.

Current PET films typically undergo a super tensilization process to raise the elastic modulus of the substrate. The chemical structure of PET, and corresponding super tensilization manufacturing process, account for a more crystalline substrate, where crystallinity refers to the degree to which the molecules are ordered or arranged. Therefore, a highly crystalline polymer will have fewer amorphous regions, and more oriented chains.

The crystallinity of PET is approximately 40%–50%, while PEN has more amorphous regions, resulting in a crystallinity of 30%–40%. Although this varies slightly with the particular test method, PET and PEN substrates have glass-transition temperatures ( $T_g$ ) of  $\sim 80$  and  $120^\circ\text{C}$ , respectively.<sup>6</sup> The glass transition temperature refers to the temperature at which the amorphous regions of a semi-crystalline material change from a glassy state to a rubbery state upon heating due to increased molecular movement.<sup>7</sup> Tape manufacturers are also producing new “advanced” substrates, such as metalized PET (M-PET) and metalized Spaltan (M-SPA), the latter being a proprietary nano-engineered PET-based material. These substrates have a thin aluminum metal layer (0.05–0.10  $\mu\text{m}$ ), which is supposed to improve the tape’s stability. Because of processing conditions, it is known to be somewhat oxidized.

### Time-Dependent Viscoelasticity: Creep and Stress Relaxation

**Fundamental Creep-Compliance Equations.** The viscoelasticity of a material refers to the combined effects of elastic and viscous deformation. Even small amounts of viscoelastic deformation can lead to long-term reliability issues with magnetic tapes such as disordered tape stacking, instantaneous speed variations, as well as tape stagger. The process known as creep strain is responsible for a significant portion of the viscoelastic deformation of magnetic tapes.<sup>2</sup> Creep experiments conducted by Bhushan and Weick generated information that has provided an insight into the understanding of magnetic tapes and their viscoelastic characteristics. A creep experiment consists of applying a constant force to a sample, while measuring the corresponding strain experienced by the sample. The creep-compliance is determined by dividing the time-dependent strain by the constant stress:

$$\varepsilon(t) = \frac{\Delta l(t)}{l_0}, \quad (1)$$

$$D(t) = \frac{\varepsilon(t)}{\sigma_0} = \frac{\Delta l(t)}{\sigma_0 l_0}, \quad (2)$$

where  $\varepsilon(t)$  is the time-dependent strain experienced by the sample,  $\Delta l(t)$  represents the change in length of the sample as a function of time,  $l_0$  is the original length of the sample,  $D(t)$  is the creep-compliance of the sample, and  $\sigma_0$  is the constant stress applied to the sample.<sup>2,7,8</sup> Creep compliance can be plotted for the duration of the experiment, providing information about the deformation characteristics of the material. The behavior of viscoelastic creep-compliance data can be modeled using the Kelvin-Voigt model, which is written mathematically as:

$$D(t) = D_0 + \sum_{k=1}^N D_k \left[ 1 - \exp\left(\frac{-t}{\tau_k}\right) \right], \quad (3)$$

where  $D(t)$  is the creep-compliance at time,  $t$ , while  $D_0$  is the instantaneous compliance at  $t = 0$ ,  $D_k$  is the discrete compliance term and  $\tau_k$  is the discrete retardation time for each Kelvin-Voigt element.<sup>2,8</sup> Note, that the retardation time represents the rate of growth of the creep-compliance curve, and can be interpreted as the length of time required to attain  $(1 - 1/e)$  or 63.2% of the equilibrium strain for each element.<sup>9</sup> The mathe-

tical equation can be represented schematically as an initial spring, which is connected in series to additional springs and dashpots in parallel.<sup>8</sup>

### Summary of Recent Creep Experiments and Relationship to Dynamic Mechanical Analysis.

Weick provides creep-compliance data for more recent tapes manufactured with PEN, PET, aramid, and metalized Spaltan substrates.<sup>8–10</sup> Attributes of the various materials are discussed to gain a better understanding of the fundamental tape and substrate characteristics. In addition, time-temperature superposition is used to predict long-term archival storage characteristics of the magnetic tape materials. This process involves fitting the creep-compliance data sets to the Kelvin-Voigt model, which generates the discrete compliance and retardation times that characterize the properties of the magnetic tape materials including the front coat, substrate, and back coat. Recently, these parameters have been used in a predictive model developed by Acton and Weick to determine deformation characteristics of the tape due to stresses imposed when the tape is stored in a reel for archival purposes.<sup>11</sup> Because of this model can be used to ultimately design future magnetic tape materials, the information is useful for tape and substrate manufacturers who need to know how their products are going to be utilized. In addition, Weick showed the importance of using substrate samples extracted from tape for creep-compliance experiments, because the properties of the substrate are affected by the processing conditions including temperature and stresses encountered during the coating process.<sup>8</sup> Finally, DMA experiments performed as part of this past research on magnetic tape materials using a commercially available device allowed for a more fundamental understanding of the substrate properties and their role in controlling dimensional stability. Therefore, it was conjectured that if DMA experiments can be performed at ultra low frequencies below the range used by commercially available DMA equipment, creep-compliance conditions can be approached. Because the underlying interpretation of DMA results is a more advanced science than the interpretation of creep-compliance experiments, ultra-low DMA experiments (or ULDMA experiments) provide a very useful source of information for the practical purpose of predicting the dimensional stability of magnetic tapes for archival storage. Furthermore, the ULDMA can utilize standard 12.7 mm (1/2 in.) tape samples cut to a 140-mm length, which makes sample preparation and installation easier than with commercial DMA equipment.

**Fundamental Stress-Relaxation Equations.** The experiments conducted with the ULDMA in this research pull a sample to a specified strain, and record the corresponding stress, and this process is repeated at three different frequencies (0.0667, 0.0333, and 0.0100 Hz), and three different temperatures (25, 50, and  $70^\circ\text{C}$ ). This action can be considered a dynamic stress-relaxation experiment, and thus, modeled with the Maxwell viscoelastic model, which consists of a spring in series with a dashpot, where the springs model the perfectly elastic elements, and the dashpots model the viscous elements.<sup>2</sup> A stress relaxation experiment is performed by pulling a sample to a specified strain, and holding the sample at that strain, while recording the stress experienced by the sample, the generalized plots of

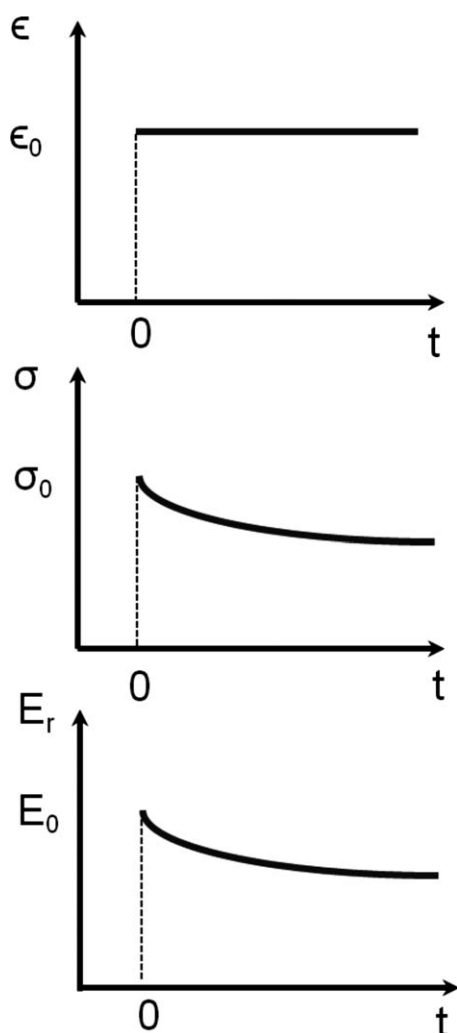


Figure 2. Maxwell relaxation experimental plots.

this are shown in Figure 2. The strain imposed on the sample is constant; therefore, the modulus of elasticity will behave similarly to the stress. The Maxwell model is expressed mathematically as follows:

$$\sigma(t) = \sigma_0 \times \exp\left(\frac{-t}{\tau_0}\right), \quad (4)$$

$$E_r(t) = E_0 \times \exp\left(\frac{-t}{\tau_0}\right), \quad (5)$$

$$\tau_0 = \frac{\eta_0}{E_0}, \quad (6)$$

where  $\sigma(t)$  is the instantaneous stress,  $\sigma_0$  is the initial recorded stress,  $\tau_0$  is the relaxation time which determines the rate of decay of the model,  $E_r(t)$  is the instantaneous relaxation modulus,  $E_0$  is the initial modulus of elasticity, and  $\eta_0$  represents the viscosity. It should be noted that the relaxation time represents the length of time required to attain  $(1/e)$  or 36.8% of the equilibrium stress for each element.<sup>9</sup> To more accurately model the relaxation of a viscoelastic material, multiple ele-

ments are typically placed in parallel, resulting in the following equation:

$$E_r(t) = \sum_{i=0}^n E_i \times \exp\left(\frac{-t}{\tau_i}\right), \quad (7)$$

for which each element has a discrete  $\tau$ ,  $\eta$ , and  $E$ . Because the elements are in parallel, the relaxation moduli are simply added together.<sup>2</sup>

#### Frequency-Dependent Viscoelasticity: Dynamic Mechanical Analysis

**Procedure.** Dynamic mechanical analysis consists of applying a sinusoidal strain to a sample, while measuring the corresponding stress experienced by the sample. This process is typically repeated cyclically, over a range of temperatures ( $-150$  to  $200^\circ\text{C}$ ) and frequencies (0.05 to 28 Hz). For a perfectly elastic material, applying a sinusoidal strain to the sample results in a completely in-phase sinusoidal stress, with the maximum stress coinciding with the maximum strain, and the minimum stress coinciding with the minimum strain. However, due to viscoelastic characteristics, magnetic tapes demonstrate a phase lag between the applied strain, and measured stress.<sup>8</sup>

The extent to which the stress signal lags behind the strain signal varies based upon the viscoelastic properties of the sample, as well as experimental parameters, such as temperature and frequency. The phase lag, or phase angle shift, can be calculated by finding the amount of time the stress signal lags behind the strain signal, and multiplying that value by the frequency of the signal:

$$\delta = \omega \Delta t = (2\pi f) \Delta t, \quad (8)$$

where  $\omega$  is the angular frequency in radians,  $f$  is the ordinary frequency in Hz,  $t$  is the time delay, and  $\delta$  is the phase angle shift in radians. Once the phase angle shift is determined, important mechanical characteristics of the magnetic tapes can be determined using the equations listed below:

$$E' = \cos(\delta) \left[ \frac{\sigma}{\epsilon} \right], \quad (9)$$

$$E'' = \sin(\delta) \left[ \frac{\sigma}{\epsilon} \right], \quad (10)$$

$$|E^*| = \sqrt{(E')^2 + (E'')^2}, \quad (11)$$

$$\tan(\delta) = \frac{E''}{E'} \quad (12)$$

If the strain applied to the sample, the corresponding stress experienced by the sample, and the phase angle shift between the strain and stress signals are known, the storage modulus ( $E'$ ), loss modulus ( $E''$ ), complex modulus ( $|E^*|$ ), and loss tangent [ $\tan(\delta)$ ] can be calculated.<sup>2,8</sup> Because of the viscoelasticity of magnetic tapes, the measured stress signal is composed of the in-phase stress, and out-of-phase stress. The in-phase component of the stress signal represents the elastically stored energy that is completely recoverable, known as the storage modulus ( $E'$ ). The out-of-phase component of the stress signal is

associated with the strain induced energy dissipation, or nonrecoverable energy that is lost to the system, referred to as the loss modulus ( $E''$ ).<sup>2,8</sup>

**Past Results for PEN, PET, and Metalized PET Tapes and Substrates.** Ma and Bhushan<sup>6</sup> used commercial DMA equipment to study PET and PEN tape and substrate samples. They showed that the storage modulus for these samples decreases with increased temperature, and decreased frequency. At higher frequencies, the storage modulus is influenced primarily by the elastic elements, while at lower frequencies, it tends to be impacted mainly by creep deformation.<sup>3,7</sup> The storage moduli of the PET samples decrease at a low rate until approximately 90°C, when the storage moduli rapidly decrease. Alternatively, the storage moduli of the PEN samples decrease at a constant rate throughout the entire experiment, at a relatively fast rate. The differences in magnitude, and rate of storage modulus decline, can be attributed to the variations in molecular structure between the polymers. The naphthalene ring in PEN is thought to be more mobile at lower temperatures than the benzene ring in PET due to the rotation of the molecule about the naphthalene ring. The lower crystallinity of PEN produces more viscoelastic characteristics, which are more dependent on temperature and frequency.<sup>3</sup>

Ma and Bhushan<sup>6</sup> also measured the loss tangent for PET and PEN samples using commercial DMA. The loss modulus represents dissipated energy, which develops as a result of the mobility of molecules in the polymer.<sup>3</sup> The loss tangents for the PET data sets are lower than those of the PEN data sets, and also peak at lower temperatures. The molecules in PEN are more mobile, especially from ambient temperature up to 60°C due to the naphthalene rings rotating along the junctions of the backbone. The temperature at which the loss tangent begins to significantly increase corresponds to the glass transition temperature of that polymer, when the movement of molecules is at its greatest.<sup>3</sup> It should also be noted that peaks in the PET data sets correspond to the temperature at which an increased rate of storage moduli decline is observed. The data sets for both PET and PEN show a shift in the loss tangent peak to lower temperatures at decreased frequencies. At higher frequencies, the molecules have a shorter period of time to respond to the strain stimulus, reducing mobility of the molecules, whereas, at lower frequencies the molecules have a longer period to respond, resulting in increased movement. Because of the mobility limitation at high frequencies, higher temperatures are needed to energize the molecules to generate movement.<sup>3,12</sup>

The data sets associated with the loss modulus tend to be overlooked; however, recent analyses performed by Weick<sup>8</sup> for PEN and metallized PET samples have provided insight into material properties that are still not completely understood. Each of the samples have a  $\beta$ -peak at a low temperature, corresponding to the short-range motions of ester groups in the backbones, and an  $\alpha$ -peak at a higher temperature, corresponding to the long-range motion in the amorphous regions, relating to the glass transition temperature.<sup>8</sup> An obvious difference between the PEN and M-PET data sets is the  $\beta^*$  peak seen at near ambient temperatures of the PEN data sets. It is believed that this peak is

unique to PEN samples because of the naphthalene ring found in the molecular structure. The rotation of the naphthalene ring results in an increase in dissipated energy. Recall that the loss modulus refers to the nonrecoverable energy that is dissipated during the experiment. Magnetic tapes are typically stored at ambient temperatures, so it is vital to understand how the material properties of the magnetic tapes influence the  $\beta^*$  peak because it is undesirable to have an energy dissipation peak occurring at storage and operating temperatures.

**ULDMA.** The ultra-low frequency dynamic mechanical analysis apparatus is comprised of six major components: force application, force measurement, displacement measurement, heat application, data collection, and data analysis. These components are integrated together in a way that produced an apparatus capable of performing dynamic mechanical analysis experiments on magnetic tape samples along temperature and frequency sweeps, while displaying all relevant data sets on an accompanied computer, along with recording the data sets into a single data file. Each of these components is discussed below, with the number in parenthesis corresponding to the number on Figure 3(a), which shows its physical location on the apparatus, and a picture of the apparatus in Figure 3(b).

The force application component of the apparatus is driven by two stepper motors (1). One end of a threaded rod is attached to each of the motors, and the other end is threaded into a platform which clamps onto the bottom of the tape sample. As the motors turn counter clockwise, the platform is raised, and when the motors turn clockwise, the platform is lowered, pulling on the tape sample. The force measurement component consists of an aluminum ring, with two strain gages attached to the inside of the ring (on opposite sides), and two strain gages attached at the corresponding locations on the outside of the ring (2). The strain gages, which act as resistors, were attached in a Wheatstone Bridge configuration. When a force is applied to the strain ring, the inside strain gages deform differently than the outside strain gages, resulting in the inside strain gages having a different resistance than that of the outside strain gages. The resistance difference results in a voltage not equal to zero across the Wheatstone Bridge. As more force is applied to the strain ring, the differences in deformation, and resistance, cause the voltage across the Wheatstone Bridge to increase. By calibrating the strain ring at different applied forces, the strain ring serves as a mechanism for measuring the stress experienced by a magnetic tape sample connected to the bottom of the ring. A Linear Variable Differential Transformer (LVDT) is connected to the platform, measuring the displacement of the magnetic tape sample, in Volts (3). A rod slides into the opening of the cylindrical LVDT, and the signal of the LVDT is dependent upon the position of the rod in respect to the bottom of the LVDT cylinder. As the platform is raised, the rod moves upward (away from the LVDT), which is recorded as an increase in voltage. On the other hand, as the platform is lowered, the rod enters further into the LVDT cylinder, registering a decrease in voltage. By calibrating the LVDT at different displacements, the LVDT will record the initial position of the magnetic tapes, along with the displacement of the tape as it is stretched to a predetermined length, allowing the strain to be calculated.

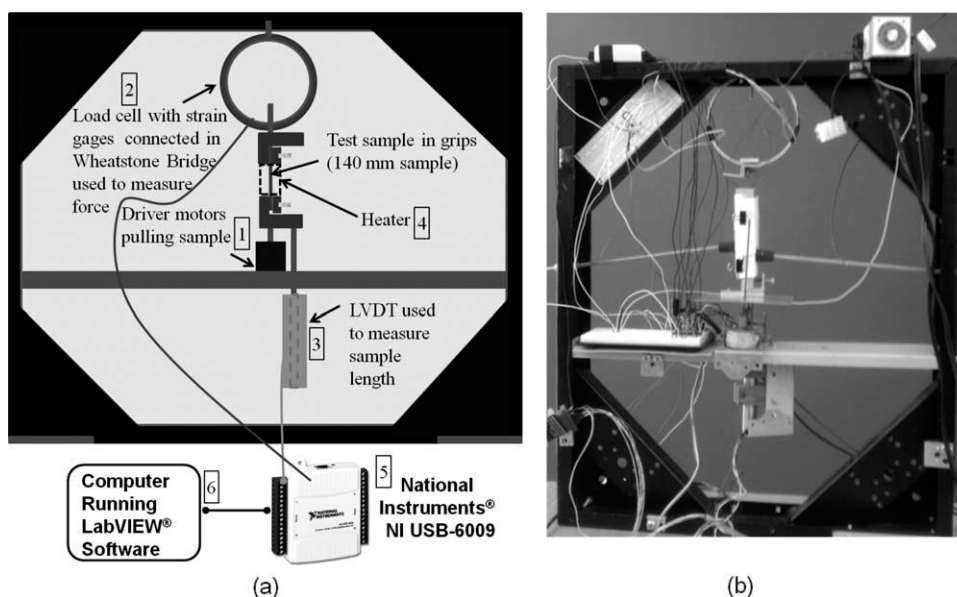


**Figure 3.** Custom ultra-low frequency dynamic mechanical analyzer (ULDMA) (a) schematic and (b) picture.

Dynamic mechanical analysis involves performing experiments along a sweep of frequencies, as well as temperatures. To account for different temperatures, a heating system has been integrated into the apparatus (4), enclosing the magnetic tape sample. The heating system is comprised of an Omron E5C2 temperature controller, two heating strips, a thermocouple, and a one-inch square aluminum channel. The two heating strips are placed on opposite, inside walls of the aluminum channel. The channel is then placed around the magnetic tape sample, with the tape equidistant from both heating strips, and the thermocouple as close to the sample as possible without touching it. This orientation allows the magnetic tape sample to be heated to a desired temperature without the other components of the ULDMA being subjected to high temperatures, which could affect their behavior. A National Instruments USB-6009 data acquisition card is used to collect data from, as well as control, all of the various components of the custom dynamic mechanical analyzer (5). The data acquisition card provides a means to communicate between the LabVIEW VIs, and the mechanical devices of the apparatus. LabVIEW software is used to control the stepper motors, as well as interpret, analyze, and display the data sets collected by the data acquisition card (6). In total, there are eight different VIs used to run experiments. Each VI has a specific purpose, such as calibrating the strain gage voltage, calibrating the LVDT, calibrating the system before an experiment, adjusting the magnetic tape holder clamps for loading a sample, loading the magnetic tape to its starting position, pre-stressing the sample, and the actual ULDMA experiment VI. Each type of magnetic tape has different physical dimensions (thicknesses), therefore, there is a separate ULDMA experiment VI for each type of magnetic tape. The ULDMA experiment VI allows the user to control the frequency of the applied strain, and the amount of applied strain. All the data are recorded and saved into a Microsoft Excel spreadsheet file, where the data set can be analyzed for more information.

The strain gages and the LVDT both record data in the form of voltages. By calibrating each of these components, the recorded values from the strain gages are converted to Newtons, while the LVDT values are converted to millimeters. The strain gages were calibrated by attaching a series of brass weights to the strain ring. The LVDT was calibrated by measuring the distance between the tape holder clamps, using a micrometer, at different values of voltages recorded by the LVDT. More information regarding the calibration of the strain gages and the LVDT can be found Rummel's thesis.<sup>13</sup>

The method by which the commercial DMA equipment determines the phase angle between the stress and strain curves is not clearly documented in manuals for the equipment. Although the fundamental theoretical equations are obviously used, calibration methods and factors to adjust for inertial effects and other machine factors are not specifically stated, making the commercial DMA equipment sometimes appear as a black box. The term black box refers to the fact that commercial DMA experiments consist of a user inputting the initial data requirements and running the experiment, then the equipment outputs all of the data, but what actually happens to the data, and how the calculations are performed, is not completely known. This article will implement the use of a fast Fourier transform program, developed by Weick, which is capable of finding the phase angle and time delay between two curves while providing the coherence between the two curves as well.<sup>14</sup> The phase angle is the value that can be used to determine the storage modulus, loss modulus, and loss tangent, as shown in eqs. (9), (10), and (12). The coherence refers to the degree to which the two signals are correlated, with zero being no correlation, and one being completely correlated. The fast Fourier transform is used to convert the discretely sampled data sets from the ULDMA experiments which are originally in the time domain,  $x(t)$ , into the frequency domain.<sup>14</sup> More in-depth information regarding this program and Fourier transforms can be found in Weick's dissertation, and Rummel's thesis.<sup>13,14</sup>

**Table I.** Thickness of Magnetic Tapes and Substrates used in Study

Sample	Description	Tape thickness ( $\mu\text{m}$ )	Substrate thickness ( $\mu\text{m}$ )
PEN	Poly(ethylene naphthalate)	6.55	5.00
PET	Poly(ethylene terephthalate)	8.00 <sup>a</sup>	6.00 <sup>a</sup>
M-PET	Metalized-PET	6.16	4.64
M-SPA	Metalized-Spaltan	6.11	4.58

<sup>a</sup>Nominal thickness.

**Test Samples.** Tape and substrate samples used in this research are shown in Table I. The PEN, metalized PET, and metalized PEN samples were provided by a corporate sponsor from the Information Storage Industry Consortium (INSIC). These are developmental tape samples, and the PEN tape is similar in composition to an LTO-4 tape. As stated previously, substrates for the metalized PET and metalized Spaltan samples have a thin aluminum metal layer (0.05–0.10  $\mu\text{m}$ ), which is supposed to improve the tape's stability. The Spaltan substrate is a proprietary nanoengineered PET-based material. Because of processing conditions, it is known to be somewhat oxidized. The PET sample is an off-the-shelf Quantum Digital Linear Tape (DLT-S4). The substrate isolation process involves rubbing both sides of the magnetic tape sample with methyl ethyl ketone (MEK), which effectively removes the front and back coat, while only the substrate remains.

### Objectives

The purpose of this research is to create a user-friendly dynamic mechanical analyzer, determine which mechanical and thermal properties can be found through ULDMA experiments, and provide an insight into how these properties vary for different magnetic tapes and substrates. Magnetic tapes are stored on reels, and are therefore subjected to stress from applied tension, bending, and compression. It is necessary to ensure that the magnetic tapes can withstand these storage forces without compromising their stability, durability, and readability.<sup>9</sup> Through ULDMA experiments, the correlation between magnetic tape material properties and magnetic tape mechanical properties will be better understood. Previous experiments have been performed using commercial DMA equipment, which provided very limited freedom to modify experimental parameters. Therefore, this research project began with the design and construction of an ultra-low frequency custom dynamic mechanical analyzer. By creating a custom ULDMA, all calculations, variables, and calibrations were created and conducted specifically for this apparatus, eliminating the black box label associated with commercial DMA equipment. Also, the apparatus was designed to require only minor adjustments to modify a variety of experimental parameters, in which the apparatus can also perform tensile tests, as well as creep tests. The development of a ULDMA was necessary to perform additional experiments at ultra-low frequencies and better understand the shifts of relaxation peaks to lower temperatures as the frequency is decreased. Furthermore, experiments conducted using the ULDMA provide

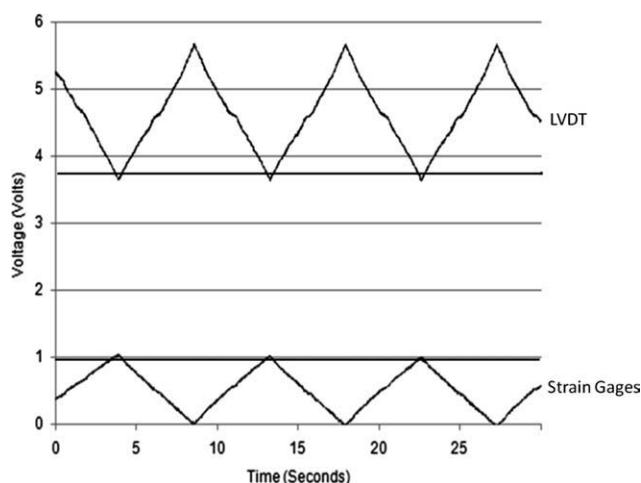
additional insight into the influence of rate and time-dependent deformation on the properties of constitutive tape materials.

## RESULTS AND DISCUSSION

### Ultra-Low Dynamic Mechanical Analyzer Raw Data

**Extraction of Elastic Modulus Data.** The primary data sets of concern from the ULDMA experiments are the strain and the corresponding stress signals. Figure 4 demonstrates an example of what the LabVIEW screen would display during an experiment (without the horizontal lines through the peaks). Note that this is just a 30-second snap shot of a 2 h experiment. Because of the orientation of the LVDT, the program was designed to have the LVDT signal appear to be opposite of the signal from the strain gages. This is because the LVDT signal will increase as the height of the platform holding the bottom of the tape sample increases, and decrease as the height of the platform decreases. Intuitively, as the height of the platform decreases, the tape sample is being stretched, and results in the maximum stress occurring at the lowest value of the LVDT signal. Therefore, the bottom peaks of the LVDT signal represent the maximum displacement of the tape, and ultimately represent the maximum strain on the tape sample, shown by the data points below the horizontal line drawn in the LVDT plot of Figure 4. Conversely, the top peaks of the signal from the strain gages represent the maximum stress, shown by the data points above the horizontal line drawn in the strain gages plot of Figure 4. The main area of interest from these data sets is the modulus of elasticity, found by dividing the stress by the strain at the maximum strain values. The data sets are filtered to only include the data points at the area of interest, which are the modulus of elasticity values near the maximum strain of each peak, and this is then plotted against the corresponding time values.

**Frequency Sweep Results.** To determine the effects of ULDMA on the magnetic tapes, experiments were performed on each of the four tape samples (PEN, PET, M-PET, and M-SPA) as well as on PEN and PET substrates with the front and back coats removed. Each type of sample underwent four ULDMA

**Figure 4.** Voltage recordings from LVDT and strain gages. Data sets acquired using the ULDMA.

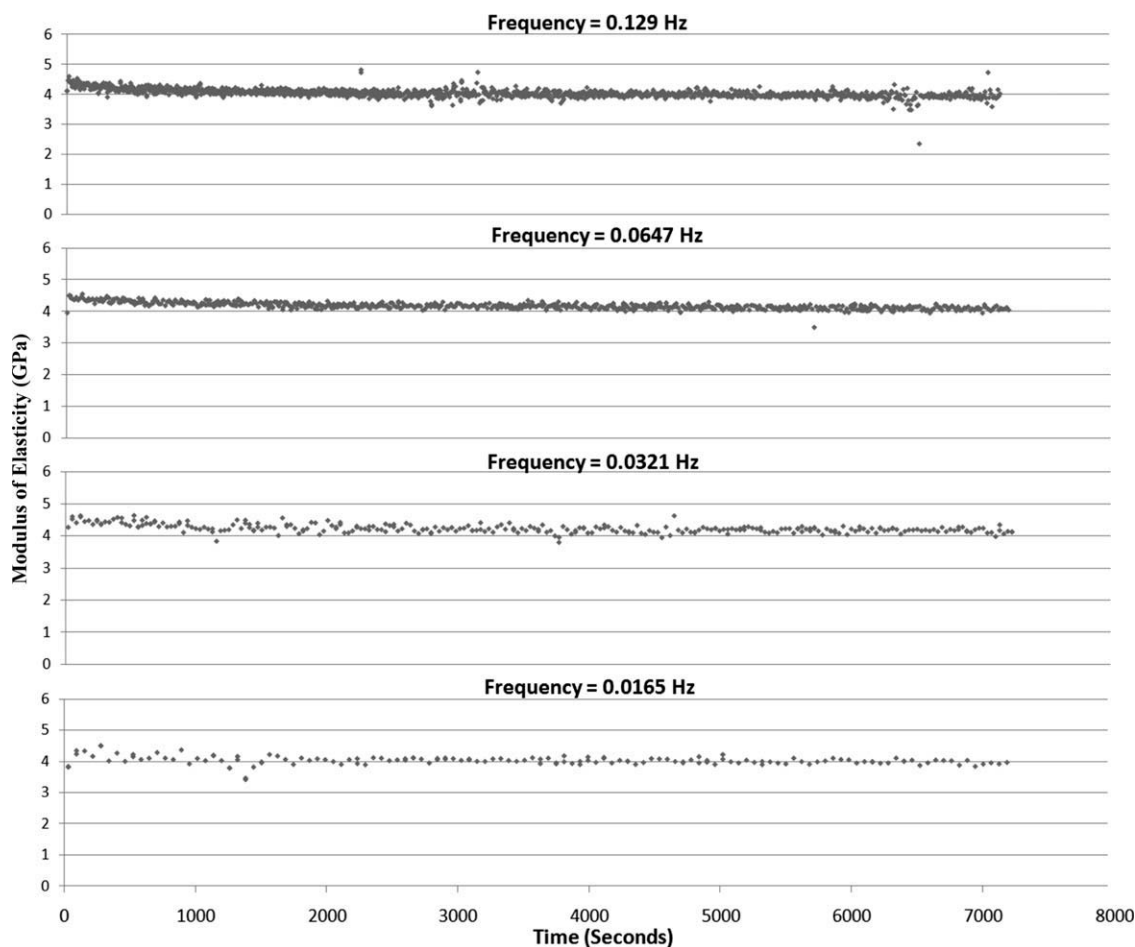


Figure 5. Frequency sweep with PEN tape from the ULDMA.

experiments, at frequencies near 0.1000, 0.0667, 0.0333, and 0.0100 Hz (Note: a new tape sample was used for each experiment). The experiments were performed at room conditions, consisting of temperatures near 25°C, and a relative humidity near 65%. The elastic moduli of the samples were calculated in LabVIEW, and plotted over the duration of the 2 h experiment with a sampling rate of 0.02 sec. The elastic moduli plots for the PEN samples are shown in Figure 5. An important feature to notice is that the modulus of elasticity is around 4 GPa, which is on the same magnitude of that found from the commercial DMA experiments. This verifies that the custom ULDMA is working properly and has been calibrated correctly. The modulus of elasticity of the PEN tape shows a slight relaxation during the first 1000–2000 sec, illustrated by a small curve in the plot. After this initial relaxation, the elastic modulus appears to remain stable throughout the remainder of the experiment. It appears that the reduction in frequency of the strain has very little or no effect on the modulus of elasticity for PEN.

The same experiments were then performed on PET tape samples, with the results shown in Figure 6. Along with a higher modulus of elasticity than the PEN tape, another noticeable difference between the two tapes is that the PET tape did not show a relaxation in the modulus of elasticity. Recall, the PET

tapes go through a tensilization process during manufacturing. This process is designed to give the PET tape a larger modulus of elasticity, which these plots confirm.

The results from the metalized PET and metalized Spaltan, Figures 7 and 8 are very similar to that of each other, and the curve resembles that of the PEN tape, as well as the magnitude of the elastic modulus. They both display the initial relaxation of the modulus of elasticity, then settle  $\sim 4$  GPa. Once again, it is interesting to note that there is no apparent decrease in elastic modulus with decreasing strain application frequency.

Because of the complexity of the layers of a magnetic tape, each layer contributes to the overall dynamic stability of the sample. To determine thermal and mechanical properties associated with the substrate of the magnetic tapes, the front and back coat were removed, and additional ULDMA experiments were performed on the substrates of PEN and PET. Figure 9 shows the results from a PEN substrate from tape sample. One of the major differences between these results and the PEN sample with the front and back coat is that the modulus of elasticity for the substrate is substantially higher. Additionally, the PEN substrate from tape does not exhibit the initial relaxation that was observed from the PEN tape with front and back coats. It is similar, however, in that the modulus of elasticity appears to remain the same as the strain application frequency is decreased.



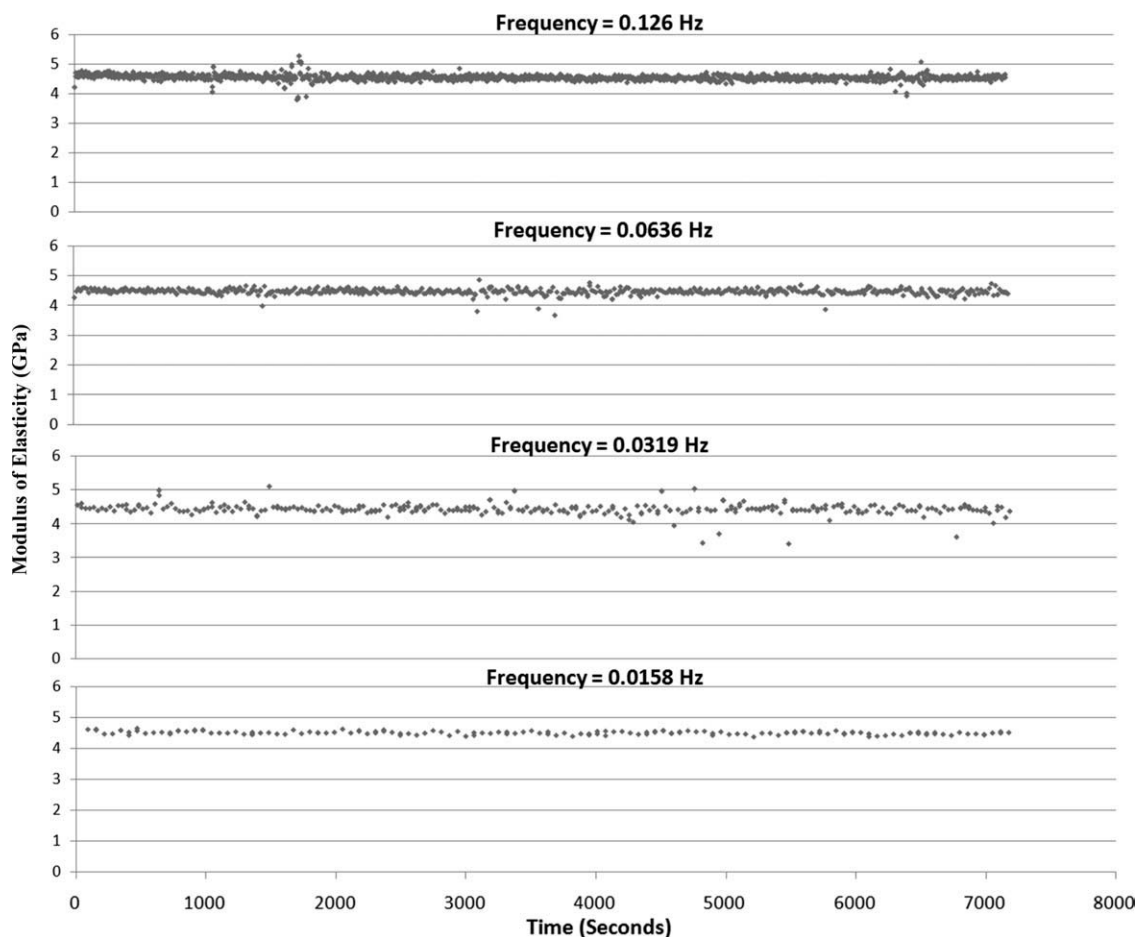


Figure 6. Frequency sweep with PET tape from the ULDMA.

Similar to that of the PEN substrate from tape, the PET substrate from tape also exhibited a higher modulus of elasticity than the PET tape with front and back coats, as shown in Figure 10. The fact that this higher elastic modulus is observed for both samples, PEN and PET, suggests that the front and back coats have some limiting effect on the modulus of elasticity of a tape sample. The PET substrate from tape shows what appears to be the opposite of a relaxation in the elastic modulus. Over the first 1000 seconds, the modulus of elasticity curves slightly upward, resulting in a final modulus of elasticity that is higher than the initial modulus of elasticity over the 2 h experiment. This trend was unexpected, and could be the result of what has been thought of for years as a shrinkage effect involving movement of partially orientated molecules in the amorphous regions at elevated temperatures.<sup>8</sup> However, recent work by Grassia and D'Amore<sup>15,16</sup> has attributed such effects to a structural relaxation phenomenon, which is a kinetics driven phenomenon involving a decrease in thermodynamic properties such as specific volume, enthalpy, and entropy. Because ultra-low frequencies tend to decrease the temperatures at which the relaxation peaks occur, it can also be argued that ultra-low frequencies decrease the temperature at which other mechanical phenomena occur. This shows that ultra-low frequencies may also contribute to the small amount of shrinkage observed for PET.

These frequency sweep experiments provided a good starting point for analyzing the different tape samples. Although the decrease in strain application frequency did not show an obvious effect on the samples when considering the modulus of elasticity, the decreased frequency may be affecting the storage modulus, loss modulus, and loss tangent. The implementation of Fourier transforms and strain–stress plot overlays were not carried out at this point in the analysis of the data. In the following sections, where the ULDMA experiments are performed along frequency and temperature sweeps, the Fourier transforms and plot overlays will provide additional valuable information. This portion of the research primarily serves as an introduction to the testing and data analysis procedure, verifying that the data recorded is both accurate and precise, as well as identifying some basic differences in the behavior of the different types of magnetic tapes and substrates when subjected to ULDMA experiments. This first section also demonstrates that the tapes and substrates undergo additional phenomena, such as stress relaxation, during the initial parts of some experiments, and even shrinkage for tensilized PET.

#### Temperature Sweep Results

The addition of a heating system to the custom ultra-low frequency ULDMA allowed the experiments to be performed along

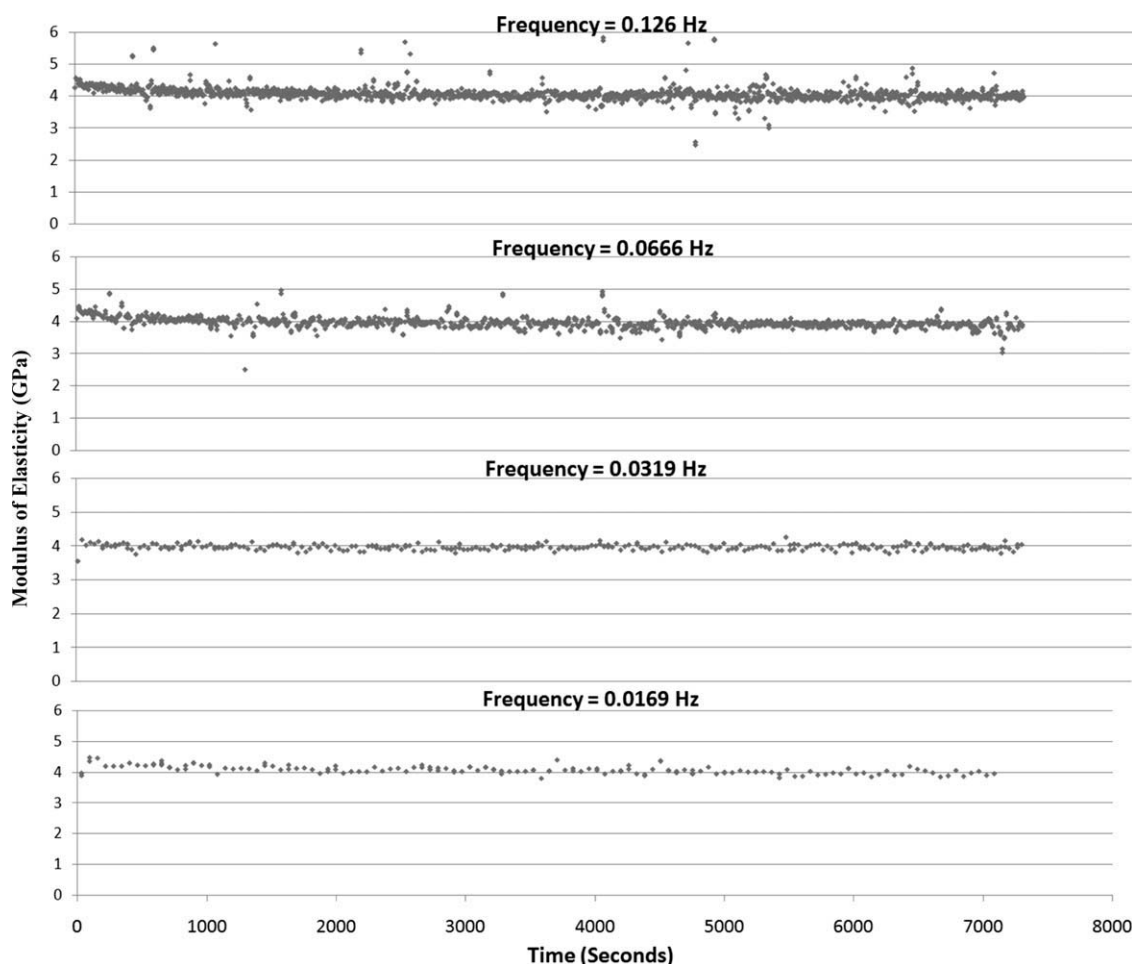


**Figure 7.** Frequency sweep with M-PET tape from the ULDMA.

temperature sweeps in addition to the original frequency sweeps. By performing experiments at different temperatures, information about the magnetic tape samples' thermal properties, such as their glass transition temperatures, could be extracted. Experiments from commercial DMAs have shown shifts in the relaxation peaks ( $\alpha$ ,  $\beta$ , and  $\beta^*$ ) to lower temperatures, associated with decreased strain application frequencies.<sup>3,6,7,17</sup> Therefore, by performing ULDMA experiments along frequency and temperature sweeps, the storage modulus, loss modulus, and loss tangent values can be plotted against temperature, demonstrating how decreased frequencies influence these peaks. Three temperatures were selected for the temperature sweep, 25, 50, and 70°C. The lower temperature limit was selected because previous DMA experiments with commercial equipment at lower frequencies have shown the loss modulus peaks shifting toward ambient temperatures. Although 50°C is the upper storage limit for magnetic tapes, performing experiments at 70°C provides relevant information about the characteristics of magnetic tapes that pertain to long-term archival storage. Additionally, three ultra-low frequencies were chosen for the frequency sweep, 0.0667, 0.0333, and 0.0100 Hz. These frequencies were chosen because the authors have determined in past research that the lowest usable operating frequency of some commercial DMA equipment is 0.0500 Hz for the test samples

used in this research. Therefore, these three frequencies will provide information near the limit of commercial DMA equipment, as well as new information at ultra-low frequencies unobtainable by some commercial DMA equipment.

Once again, all of the data points except those relevant values at the peaks of the strain and corresponding stress values were filtered out, allowing the modulus of elasticity to be calculated at the maximum strain of each cycle. The modulus of elasticity for each of the three temperatures was plotted against time for the duration of the 2-h experiment. While each experiment was only performed one time, the repeatability of these experiments can be verified by comparing the original frequency sweep plots with those of the temperature sweeps at 25°C. Figure 11(a), shows the results of the PEN tape sample at the three frequencies, whereas Figure 11(b), shows the results of the PET tape. As demonstrated before in the frequency sweeps, the PEN tape once again has an initial relaxation. This initial relaxation becomes increasingly apparent at elevated temperatures. The decreased strain application frequency appears to have very little, or no effect, on the modulus of elasticity. Conversely, the increase in temperature has a drastic effect on the modulus of elasticity, dropping the elastic modulus approximately 2 GPa from 25 to 70°C. The elastic modulus of PET, on the other hand, is less affected by

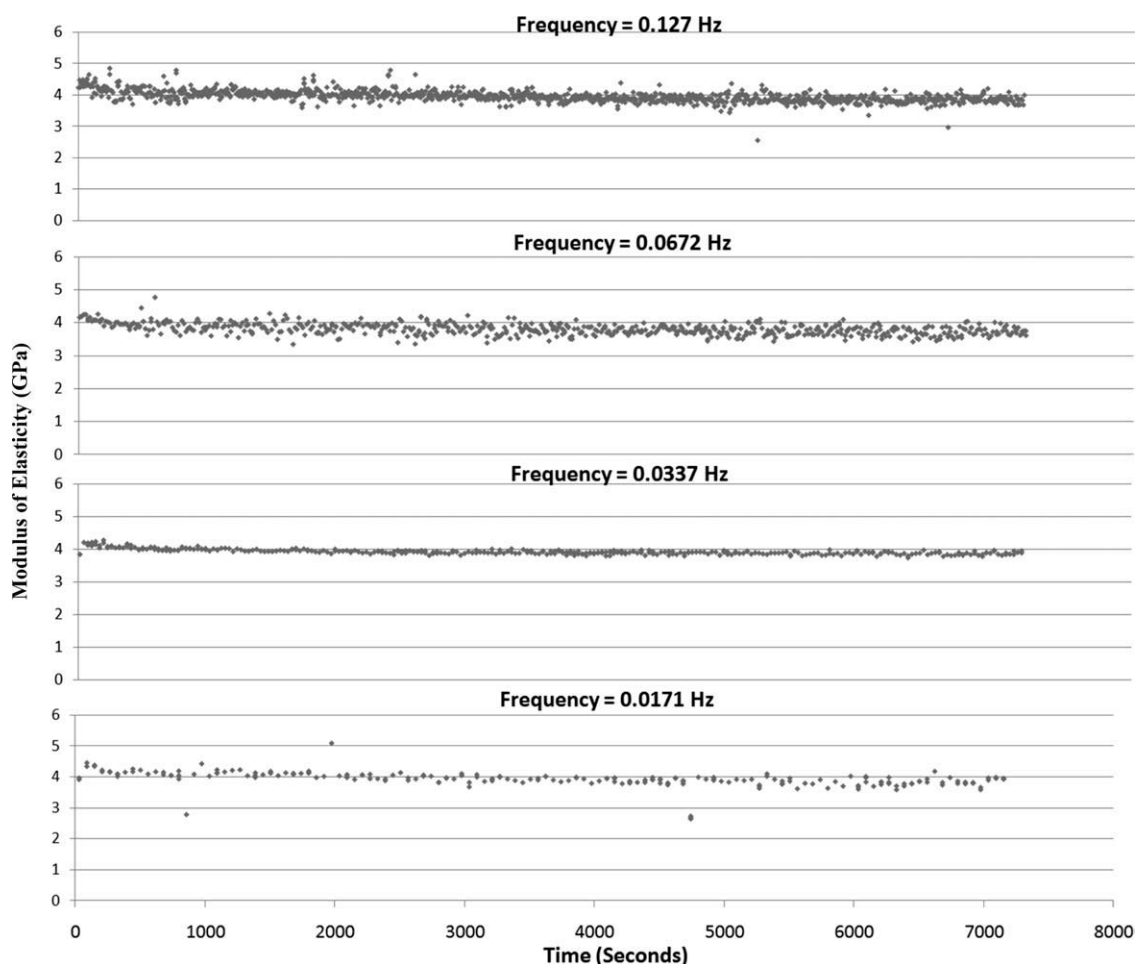


Figure 8. Frequency sweep with M-SPA tape from the ULDMA.

temperature, decreasing nearly 1.5 GPa 25 to 70°C. As seen with the frequency sweeps, the PET samples do not show the initial relaxation at the lower temperature, however, at elevated temperatures a significant relaxation curve is present. Also, the modulus of elasticity of PET is higher than that of PEN at each corresponding combination of temperature and frequency.

The temperature sweep experiments were repeated using M-PET and M-SPA samples. While the frequency sweep plots of these two samples were nearly identical, it is desirable to determine whether the two samples will display different elastic modulus properties at elevated temperatures. The results from the metalized PET ULDMA experiment are shown in Figure 12(a), while those from metalized Spaltan are shown in Figure 12(b). Once again, the plots of these two samples resemble that of each other, as well as that of the PEN tape. Both of the samples demonstrate the initial relaxation in the elastic modulus, which becomes increasingly pronounced as the temperature is increased. Also, the change in the modulus of elasticity is much more affected by increased temperature than decreased strain application frequency. However, unlike the PEN samples, the modulus of elasticity only decreases 1.5 GPa from 25 to 70°C. It appears as though both, frequency and temperature, have the same effect on the elastic modulus properties of M-PET and M-SPA.

Finally, the temperature sweep ULDMA experiments were performed on PEN substrates from tape, as shown in Figure 13(a), as well as the PET substrates from tape, as shown in Figure 13(b). As expected, there was a much more noticeable elastic modulus relaxation at the elevated temperatures for both samples. The linear portion of the elastic modulus for the PEN substrate from tape was higher than that of the PEN sample with front and back coats, but similar in that the elastic modulus dropped approximately 2 GPa from 25 to 70°C. The modulus of elasticity of the PET substrate from tape was higher than that recorded for the PET sample with front and back coats, as well as the PEN substrate from tape. As seen with the PEN and PET samples with front and back coats, the modulus of elasticity of the PEN and PET substrates from tape did not appear to be affected by the decrease in strain application frequency.

While the plots of the modulus of elasticity provide valuable information highlighting how different magnetic tapes samples react to ULDMA experiments, much more information can be gathered by determining the presence of a phase lag between the strain and corresponding stress signals. These plots have merely shown how the elastic modulus is affected by temperature and frequency, providing an insight in the viscous versus elastic behavior of the samples. However, by determining phase

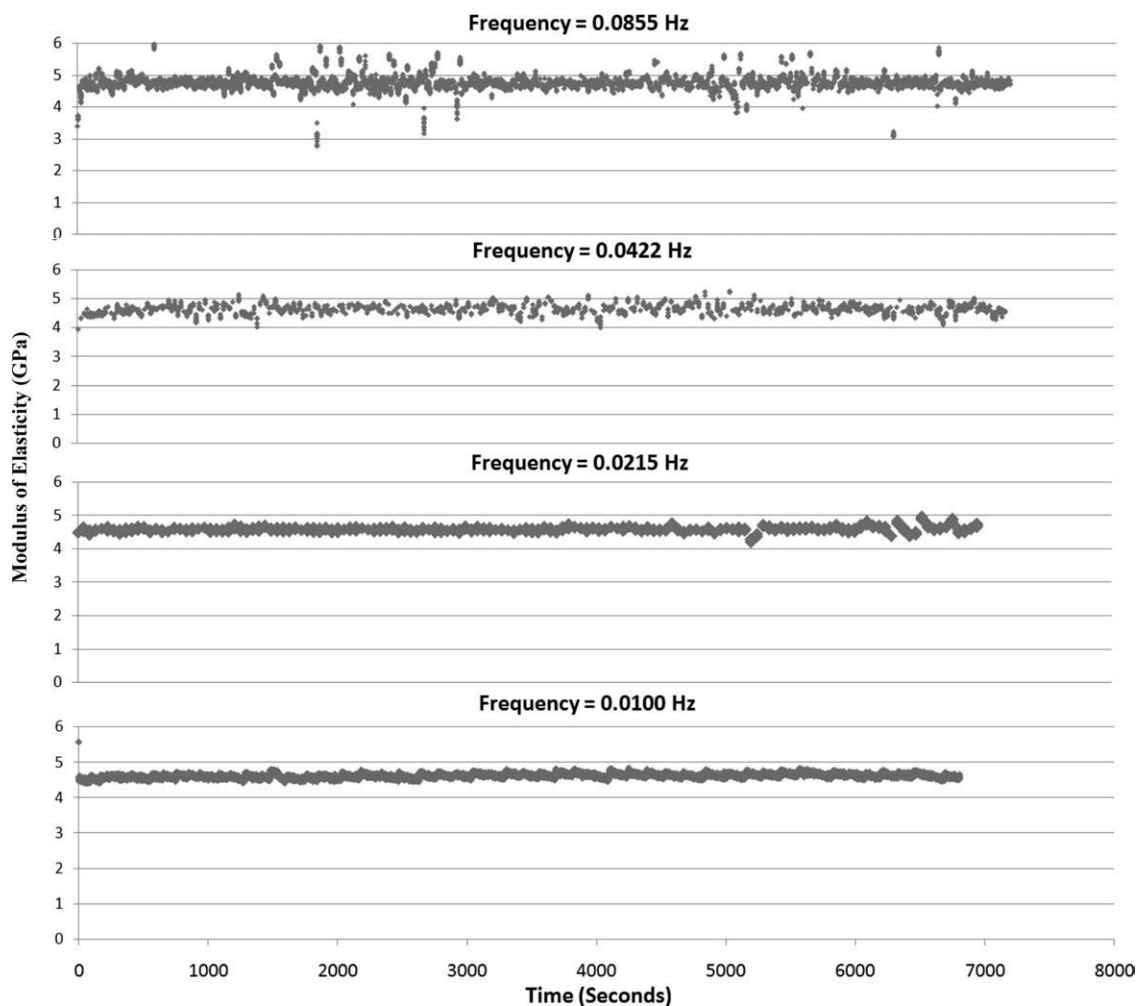


**Figure 9.** Frequency sweep with PEN substrate from tape acquired with the UDMA.

angles and time delays, additional information regarding dissipated energy and relaxation peaks resulting from molecular movement.

**Determination of Phase Angles and Time Delays Overlay of Strain and Stress Plots, and Fourier Transform Analysis.** One way to determine whether a time delay exists is to overlay the strain and stress plots. The idea behind this method is that as the magnetic tape is stretched, the stress signal lags behind the strain signal due to molecular movement in the polymers. Therefore, this time delay will result in the maximum stress occurring just after the maximum applied strain. This overlay technique is difficult to implement because the time delay between the two signals can be very small, to within tenths or even hundredths of a second, resulting in a shift that would be very difficult to discern with a plot overlay.

A more effective way to determine the existence of a phase lag is the use of Fourier transforms. This technique involves converting the discretely sampled data from the time domain into the frequency domain. By inputting the strain and stress signals (unfiltered) into the Fourier transform program developed by Weick, a data set is generated with phase angle and time delay

information, along with the coherence between the two signals at frequencies of zero up to the Nyquist Frequency.<sup>14,18</sup> The coherence signal is highest at the lower frequencies, and drops to near zero from 0.1000–1.000 Hz. At the strain application frequency, the coherence of the strain and stress signals approaches 1, meaning the two signals are completely correlated, and the corresponding phase angle and time delay values accurately reflect the actual phase angle and delay between the strain and the stress plots. Recall from eq. (8) that the time delay is related to the phase angle by dividing the phase angle by the strain application frequency and multiplying by  $2\pi$ .

The phase angle and time delay of each of the samples are shown in Table II. Note that the phase angle and time delay values are negative due to the fact that the stress signal is lagging behind the strain signal. Although there are only nine data points for each tape sample, the table provides valuable information regarding the trends of different tapes at various combinations of frequency and temperature. The most noticeable trend for each of the samples is that the time delay substantially increases as the frequency is decreased. This is important to note, because while the decrease in frequency did not appear to have an effect on the elastic modulus when looking at the

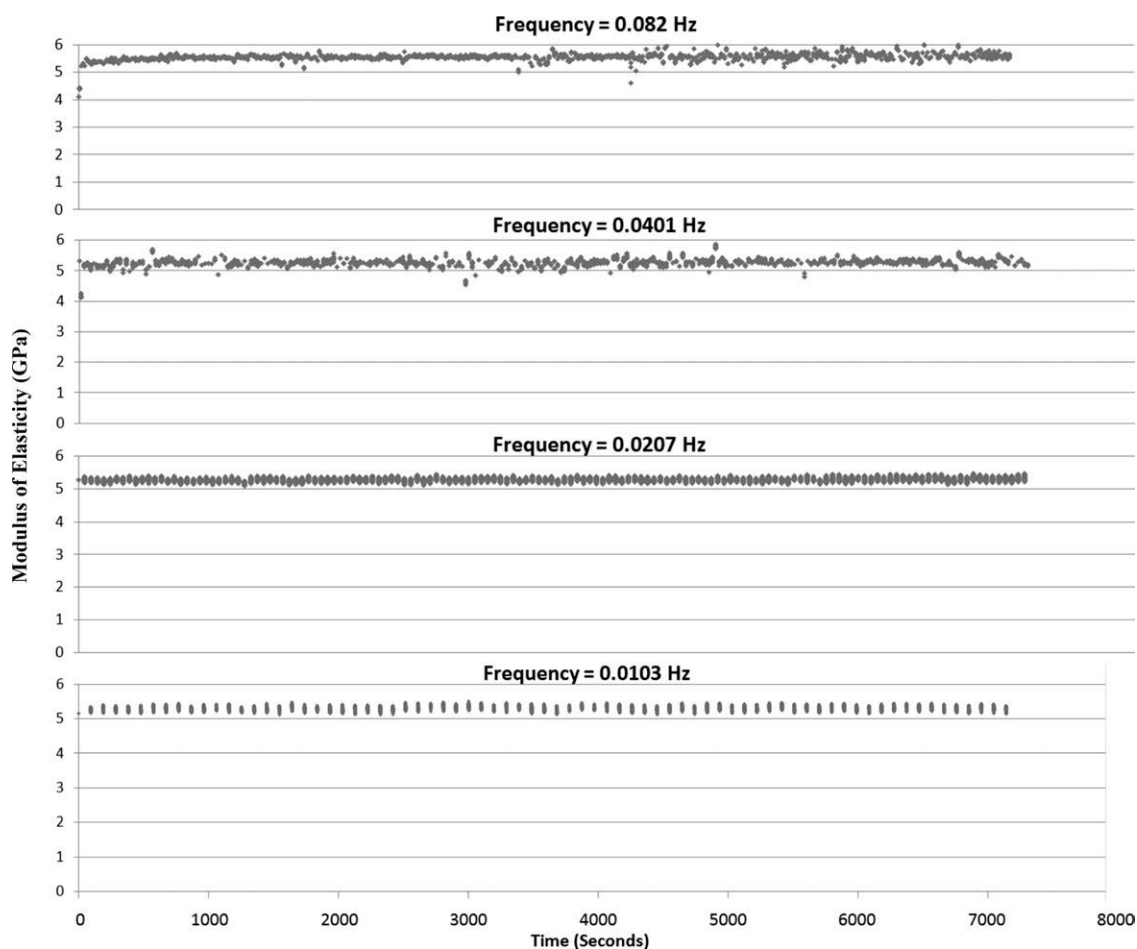
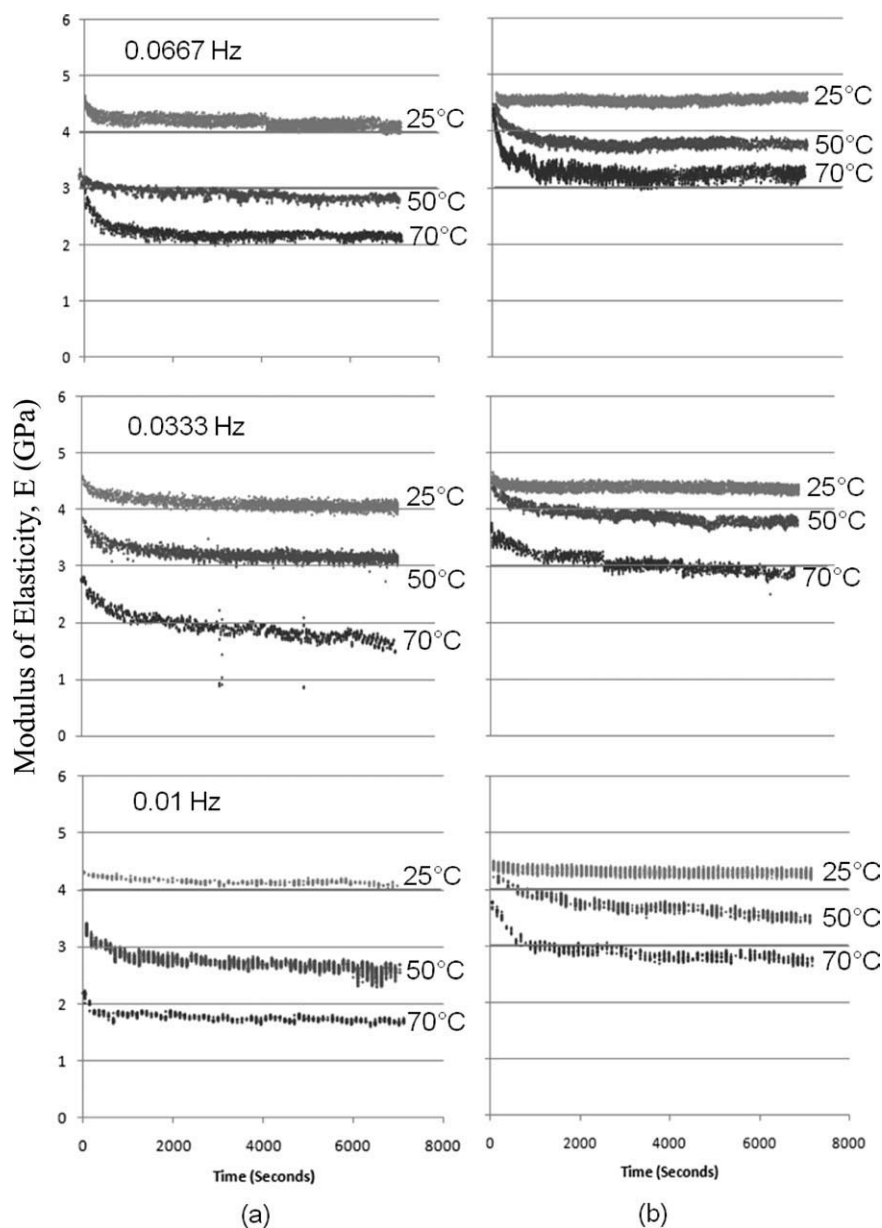


Figure 10. Frequency sweep with PET substrate from tape acquired with the UDMA.

previous plots, this table shows that decreased frequency increases the time delay. Another trend that is apparent in each of the samples is that the time delay values are higher at 50 and 70°C than at 25°C. However, the highest time delay values are not consistently at the highest temperature for each frequency. For example, the highest time delay for the PEN sample at 0.0100 Hz is at 50°C, while the highest value for 0.0333 Hz and 0.0667 Hz is at 70°C. The cause for this will be more clearly understood as the storage modulus, loss modulus, and loss tangent are determined. The time delay values for the PET samples are lower than their corresponding values for PEN. Similarly, the PET substrate from tape has time delay values that are lower than the values for the PEN substrate from tape. Additionally, the time delay values of the PEN and PET substrates from tape are lower than their respective tapes with the front and back coats. Although the elastic modulus plots for M-PET and M-SPA samples appeared to be nearly identical, the time delays for the M-PET samples, specifically the 0.0100 and 0.0333 Hz at 70°C, are noticeably lower than the corresponding values of the M-SPA samples. These differences between M-PET and M-SPA have gone unnoticed in past experiments with commercial DMA, because they occur below the usable frequency range of that equipment for the magnetic tape materials in the study.<sup>8</sup> Because the differences are due to transitions, the magnitude

and location of the transition peaks on a temperature scale do not necessarily shift consistently with frequency, which disables the accurate use of frequency-temperature shifting to predict the presence of these peaks using higher temperature experiments corresponding to lower frequencies.<sup>8</sup> While the time delay values appear to be more distinct in distinguishing the differences between samples, the phase angles actually provide even more valuable information. Recalling the eqs. (9)–(12), the storage modulus, loss modulus, and loss tangent can be determined from the phase angle.

**Storage Modulus, Loss Modulus, and Loss Tangent Analysis.** Figure 14(a,b) show the plots of the storage modulus, loss modulus, and loss tangent for PEN and PET tape samples, respectively. When comparing the storage modulus plots for the PEN and PET tape samples, the rate of decrease for the PEN tape samples is noticeably steeper than that of the PET tape samples. The modulus of elasticity is decreasing approximately 2 GPa from 25°C to 70°C for PEN, a slope of  $-0.0467$  GPa/°C, while PET is only decreasing about 1.5 GPa, a slope of  $-0.0333$  GPa/°C. The differences in slope and change in storage modulus can also be related to the magnitude of the loss tangent. The loss tangent is the ratio of viscous, or unrecoverable dissipated energy over the recoverable elastic energy during deformation of



**Figure 11.** (a) Temperature sweep with PEN tape and (b) temperature sweep with PET tape. Data sets acquired using the UDMA.

the sample. A viscoelastic polymer will dissipate a significant amount of energy upon deformation, compared with an elastic polymer, and result in a higher loss tangent. The higher loss tangent values for PEN correspond to a steeper storage modulus slope, suggesting that the PEN tape sample is more viscoelastic than the PET sample. Also, the storage modulus values for PET are greater than those of PEN, suggesting that PET has better elastic stiffness properties. The elevated stiffness is due to the amount of crystallization in PET, where PET has more crystalline regions than PEN, and is comprised of more oriented chains.<sup>8</sup> Specifically for PET, these polymeric chains are anchored down and less mobile, reducing the amount of deformation caused by an applied strain.<sup>19</sup> Amorphous regions are more temperature and frequency dependent than that of crystalline regions, which is evident by the PEN samples having a

lower storage modulus, along with a steeper storage modulus slope. Also, the tensilization process with PET increases the amount of stress needed to cause molecular movement. However, the tensilization process builds up residual stresses, which begin to relax at elevated temperatures, and release unrecoverable energy, resulting in higher loss tangent values, steeper storage modulus slopes, and can lead to shrinkage.<sup>2,8</sup>

Previous experiments conducted with commercial DMA equipment have shown these trends, as the storage modulus slope is fairly stable until it reaches an elevated temperature near 100°C, when more energy is released, and the slope of the elastic modulus becomes more negative.<sup>3,6–8,17</sup> This is also reflected in the loss tangent plots, where the peak of the  $\alpha$ -peak aligns with the temperature at which the storage modulus slope changes. The plots of the loss modulus for PEN show a peak for the ultra-low

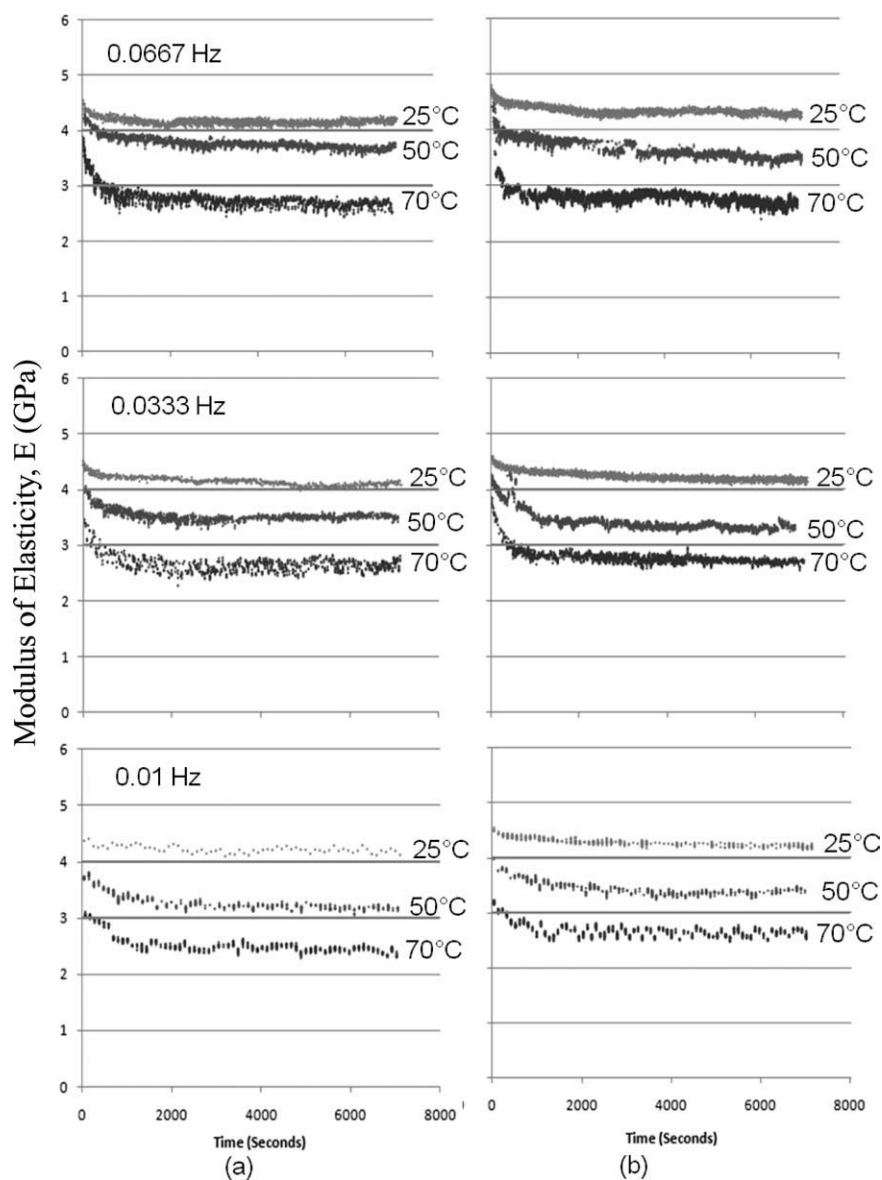


**Figure 12.** (a) Temperature sweep with M-PET tape and (b) temperature sweep with M-SPA tape. Data sets acquired using the UDMA.

0.0100 Hz frequency at 50°C, and this same trend is shown for the 0.0100 Hz frequency at 50°C for the loss tangent. The fact that this peak, which represents dissipated energy, occurs at 50°C and lower is important because 50°C is an upper design temperature for magnetic tapes. Additionally, even if it is stored at a lower temperature, the behaviors observed at the 50°C temperature can occur after longer periods of time due to the viscoelastic characteristics of PEN.<sup>10</sup> However, this peak is not present in either of the loss modulus or loss tangent plots associated with the PET samples. The fact that this peak is present in the PEN samples but not PET samples suggests that it is due to the  $\beta^*$  peak, which has not been observed for PET samples in prior experiments performed with commercial DMA equipment.<sup>8</sup> The presence of the  $\beta^*$  peak is most likely due to the relative motion of the naphthalene ring in the polymer chain of PEN.<sup>20</sup> These secondary motions are a form of energy dispersion, which, as previously mentioned, results in the steeper storage modulus slope.

The additional energy released in PEN resulting from the mobility of the naphthalene ring is the reason that the elastic modulus slope of PEN is more negative than that of PET. Because of the absence of a naphthalene ring in PET, there are fewer secondary motions, and less energy is dissipated. Moreover, the loss modulus plots for PEN show that the  $\beta^*$  peak is shifting toward a lower temperature as the strain application frequency is reduced. This shift can be attributed to the amount of time the molecules have to respond to the applied stress. At low strain application frequencies, the molecules have a longer time to respond to an applied strain, whereas with high strain application rates, the molecules have less time to react. Therefore, at higher frequencies a higher temperature is needed to energize the molecular movement, which is why the relaxation peaks shift to higher temperatures as the frequency is increased.

The corresponding plots for M-PET and M-SPA are shown in Figure 15(a,b), respectively. The M-PET and M-SPA storage

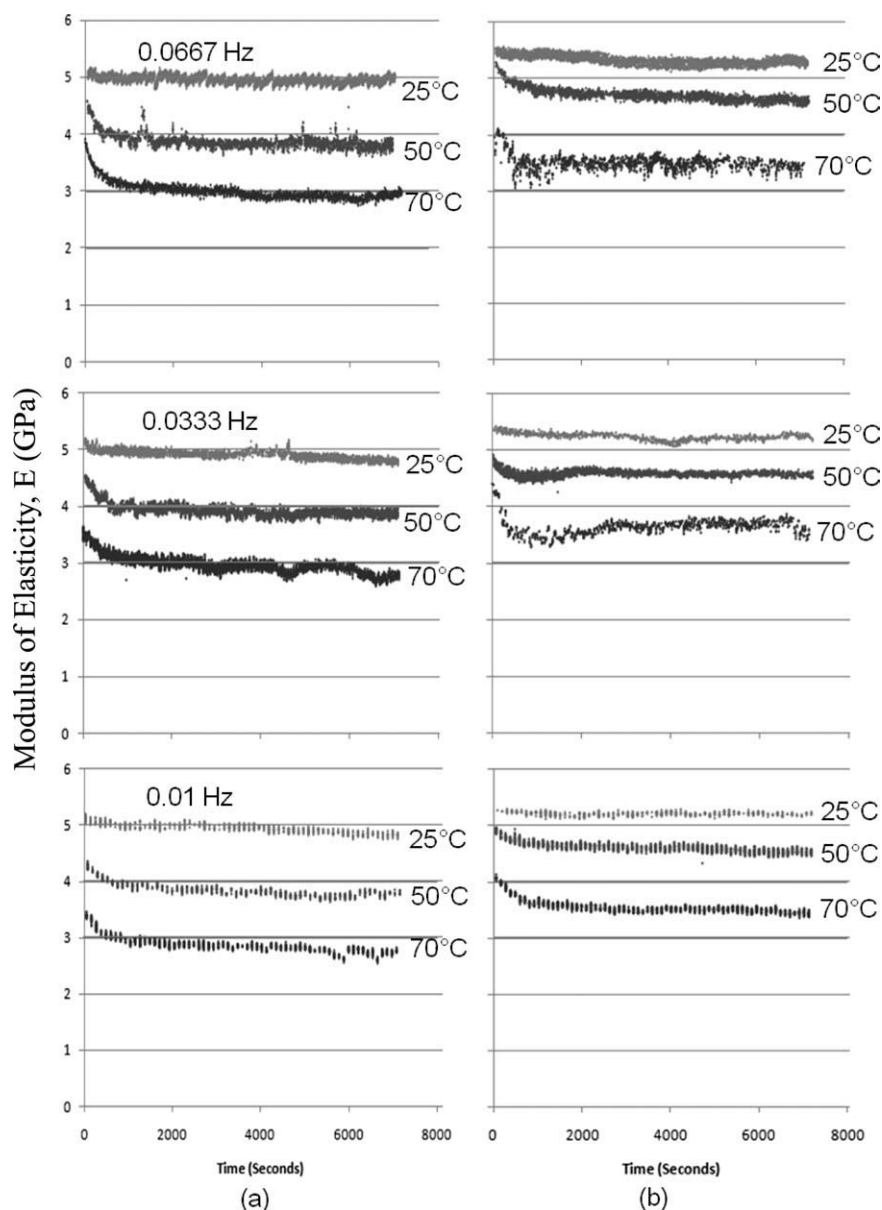


**Figure 13.** (a) Temperature sweep with PEN substrate from tape and (b) temperature sweep with PET substrate from tape. Data sets acquired using the ULDMA.

modulus plots are very similar to each other with regards to the values and trends of the elastic modulus. The storage modulus decreases approximately 1.5 GPa over the temperature sweep, a slope of  $-0.0333$  GPa/ $^{\circ}$ C, resembling that of PET, suggesting that these metalized samples are more elastic than the PEN samples. This is also supported by the lack of a  $\beta^*$  peak in the loss modulus plots, suggesting less secondary molecular movement. A slight increase in the low frequency, high temperature values is noticeable in the loss modulus plots, and much more apparent in the loss tangent plots. This increase at elevated temperatures can be assumed to be leading into the  $\alpha$ -peak, representing the glass transition temperature, which is occurring at lower temperatures than the PEN and PET tapes. The magnitude of the 0.0333 Hz, 70°C data value for M-SPA is unexpectedly higher than that of the corresponding temperature at

0.0100 Hz in the loss modulus and loss tangent plots. At this point it is unclear whether this anomaly was an experimental error, or if the molecular structure of M-SPA has a frequency threshold at which the relaxation peaks shift to lower temperatures. Because Spaltan is a nanoengineered polymer blend, this anomaly could be due to the other unknown polymer that is blended with PET. Additionally, this shows the importance of performing additional ULDMA experiments on these samples at more temperatures, generating plots with more data points which would more clearly show the relaxation peaks.

The plots of the PEN and PET substrates from tapes are shown in Figure 16(a,b), respectively. The storage modulus plots for each of the two samples show a similar downward trend, with the one difference being that the values of the PET substrate



**Table II.** Phase Angles and Time Delays of Each Tape Sample

	Frequency (Hz)	Temperature (°C)	Phase angle (Rads)	Time delay (s)
PEN	0.0667	25	-0.1071	-0.2567
		50	-0.1205	-0.2888
		70	-0.1202	-0.2880
	0.0333	25	-0.1045	-0.5010
		50	-0.1178	-0.5648
		70	-0.1233	-0.5912
	0.0100	25	-0.1093	-1.781
		50	-0.1954	-3.184
		70	-0.1288	-2.099
PET	0.0667	25	-0.0816	-0.1955
		50	-0.0787	-0.1886
		70	-0.1022	-0.2449
	0.0333	25	-0.0844	-0.4044
		50	-0.0897	-0.4298
		70	-0.1080	-0.5178
	0.0100	25	-0.0831	-1.355
		50	-0.1141	-1.859
		70	-0.1088	-1.770
M-PET	0.0667	25	-0.1121	-0.2688
		50	-0.1256	-0.3009
		70	-0.1385	-0.3320
	0.0333	25	-0.1129	-0.5411
		50	-0.1310	-0.6279
		70	-0.1457	-0.6985
	0.0100	25	-0.1093	-1.781
		50	-0.1377	-2.244
		70	-0.1870	-2.564
M-SPA	0.0667	25	-0.1148	-0.2752
		50	-0.1238	-0.2967
		70	-0.1299	-0.3113
	0.0333	25	-0.1040	-0.4983
		50	-0.1392	-0.6672
		70	-0.2227	-1.068
	0.0100	25	-0.1179	-1.922
		50	-0.1435	-2.339
		70	-0.1887	-3.076
PEN substrate from tape	0.0667	25	-0.1066	-0.2555
		50	-0.1212	-0.2992
		70	-0.0962	-0.2240
	0.0333	25	-0.1028	-0.4928
		50	-0.1091	-0.5232
		70	-0.0987	-0.4732
	0.0100	25	-0.0963	-1.569
		50	-0.0999	-1.628
		70	-0.1000	-1.630

**TABLE II.** Continued

	Frequency (Hz)	Temperature (°C)	Phase angle (Rads)	Time delay (s)
PET substrate from tape	0.0667	25	-0.0725	-0.1739
		50	-0.0823	-0.1971
		70	-0.0823	-0.1971
	0.0333	25	-0.0715	-0.3427
		50	-0.0779	-0.3735
		70	-0.1082	-0.5187
	0.0100	25	-0.0613	-0.9993
		50	-0.0919	-1.497
		70	-0.0864	-1.409

from tape are higher than those of the PEN substrate from tape. The substrates for each tape showed a similar effect due to temperature as their respective tapes with front and back coats. PEN decreased nearly 2 GPa, while PET decreased 1.5 GPa from 25 to 70°C, with slopes of -0.0467 and -0.0333 GPa/°C, respectively. Both samples have higher values of storage modulus than their respective tapes with front coat and back coat. A possible reason that tape samples with front and back coats have a lower storage modulus is because they are composed of layers, acting as a composite material. Because of this, the bonds at the interface are likely to be less stable than those within each layer, so energy is dissipated at the interface as a strain is applied. A more significant difference in the two samples is apparent in the plots of the loss modulus and loss tangent. The PEN substrate from tape shows a peak at 25°C for each of the frequencies in the loss modulus plot. This peak is not present in the PET substrate from tape plot, as it represents the  $\beta^*$  peak. Similarly, a small peak is visible in the loss tangent plots for the PEN substrate from tape, whereas the PET substrate from tape values appear to be increasing, leading into the  $\alpha$ -peak. The cause for the differences between the PEN and PET substrates from tape is the same as for the differences between the PEN and PET tapes with front and back coats. The molecular differences between PEN and PET cause the PEN substrate from tape to behave more viscoelastically, apparent in the steeper storage modulus slope, the presence of a  $\beta^*$  peak in the loss modulus plot, and larger values for the loss tangent plot. However, the  $\alpha$ -peak for the PET samples, corresponding to the glass transition temperature, is lower than PEN samples, demonstrating PEN's superior thermal properties at elevated temperatures.

**Relaxation Curve Analysis.** Another method of analyzing the ULDMA results of the magnetic tapes samples is to model the relaxation curves with a single element Maxwell viscoelastic model. The relaxation times can be calculated progressively throughout the ULDMA experiment results, showing the extent to which the relaxation curves mimic those of a Maxwell model. The relaxation time represents the rate of decay of the viscoelasticity, and is the time at which the relaxation modulus is equal

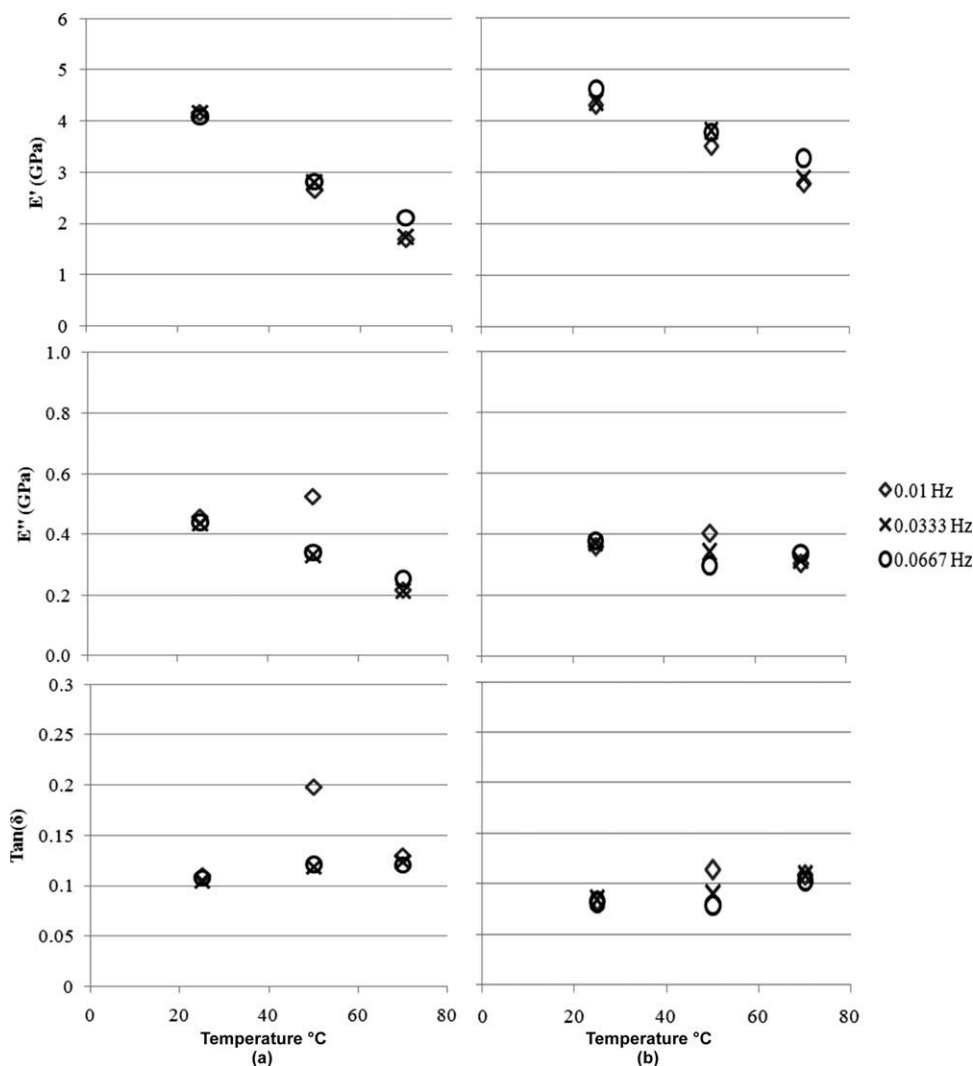


**Figure 14.** Storage modulus ( $E'$ ), loss modulus ( $E''$ ), and loss tangent [ $\tan(\delta)$ ] for (a) PEN and (b) PET tape samples. Data sets acquired using the ULDMA.

to approximately 37% of the initial modulus of elasticity. The steps for finding the relaxation times are demonstrated below:

$$E_r(t) = E_0 \times \exp\left(\frac{-t}{\tau_0}\right), \quad (13)$$

$$\ln\left(\frac{E_r(t)}{E_0}\right) = \frac{-t}{\tau_0}, \quad (14)$$

$$\tau_0 = \frac{-t}{\ln\left(\frac{E_r(t)}{E_0}\right)}, \quad (15)$$

where  $\tau_0$  is the relaxation time for the single element Maxwell model. By implementing eq. (15) at four different times (250, 500, 1000, and 2000 sec) with the initial modulus of elasticity,  $E_0$ , and the relaxation modulus,  $E_r$ , at each of these times, Table III was generated. This table can be interpreted by associating smaller relaxation times with larger relaxation curves, which represents viscous behavior. The four different times (250, 500, 1000, and 2000 seconds) were chosen to show how the relaxa-

tion of the sample changes throughout the experiment. It would be expected that a more viscoelastic material would have lower relaxation times, because the relaxation time relates to how quickly the elastic modulus decays. Therefore, if a sample is very viscoelastic, it would have a very large curve, decay at a fast rate, and have a small relaxation time. Alternatively, a very elastic material would not dissipate very much energy, or generate a relaxation curve, and would therefore have a very stable elastic modulus. Because there is no relaxation curve, an elastic material would not be modeled correctly using a one element Maxwell model, demonstrated with relatively high relaxation times. These concepts are verified in the table, where the PEN tapes show smaller relaxation times than PET. This once again reinforces the notion that PEN behaves more viscoelastically, while PET behaves more elastically. Additionally, it would be expected that because the relaxation time would be larger as the experiment progress because the slope of a curve decreases further along the curve. This belief is verified for each sample, where the curve is much more prevalent at the beginning of the

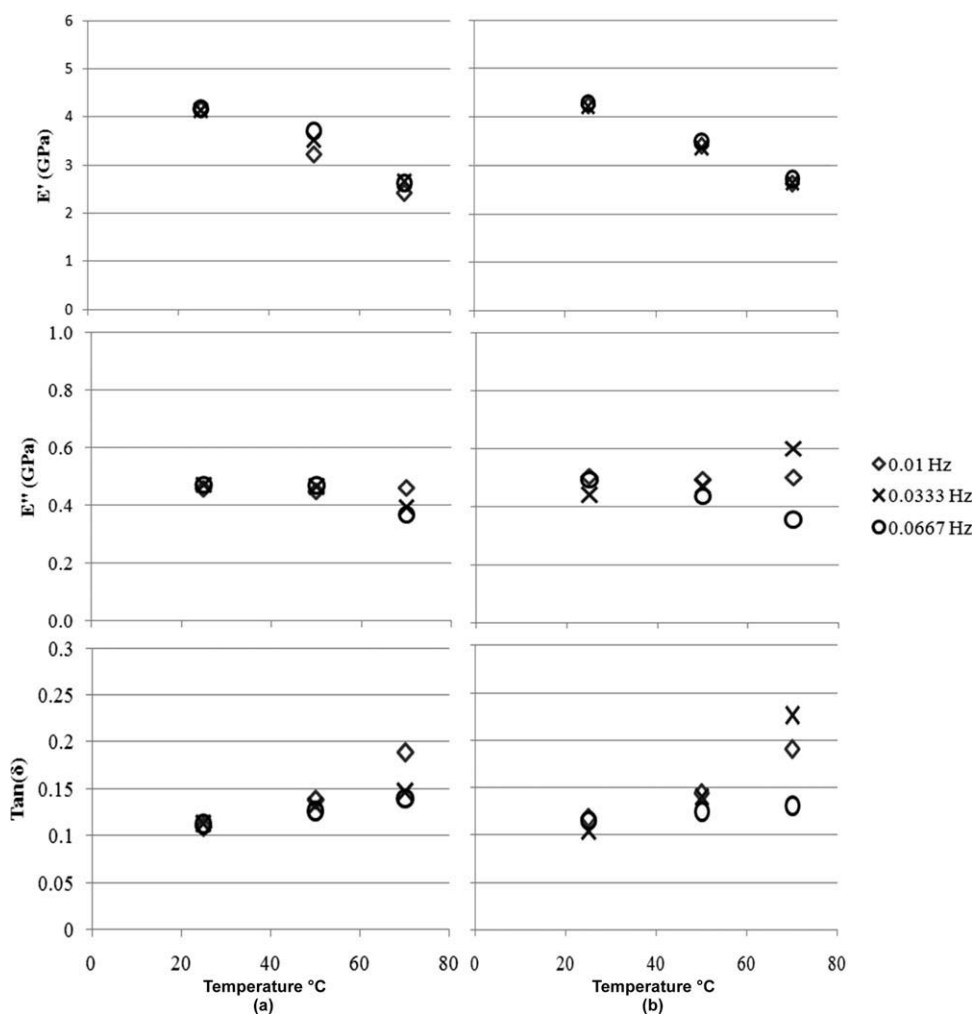


**Figure 15.** Storage modulus ( $E'$ ), loss modulus ( $E''$ ), and loss tangent [ $\text{Tan}(\delta)$ ] for (a) M-PET and (b) M-SPA. Data sets acquired using the UDMA.

experiment, then levels off as the experiment proceeds, resulting in the smallest relaxation time occurring at 250 sec, and the largest relaxation time occurring at 2000 sec.

All of the samples show some common trend, one being as the temperature is increased, the relaxation time decreases. Also, as the strain application frequency is increased, the relaxation times tend to decrease. However, it is evident that the increase in temperature has a greater effect than the increase in frequency, reflected by a greater change in relaxation times resulting from an increase in temperature. Although counterintuitive compared with the typical temperature and frequency relationship for viscoelastic behavior, when modeled as a single element Maxwell model at elevated temperatures and elevated frequencies, magnetic tapes exhibit much more viscous characteristics than they do at lower temperatures and frequencies. Also, notice that the PEN and PET substrates from tape displayed very little or no relaxation at 25°C. This lack of relaxation is verified with relatively high relaxation times at 25°C. Recall from the storage modulus, loss modulus, and loss tangent plots that the PEN samples behaved more viscoelastically than the PET samples. This trend is supported by Table III, where at 25°C, the relaxa-

tion times associated with PEN are lower than those of PET, and the same trend is seen for the PEN substrates from tape compared to the PET substrates from tape.

The decline in relaxation times over the duration of the experiment is clearly visible in Figure 17, which shows a plot of the original modulus of elasticity data set for M-SPA with 0.0667 Hz at 50°C, along with the data modeled after each of the relaxation times from Table III. A material that follows the single element Maxwell model would have a very large curve leveling off near zero at the end of the 7200-min experiment. Therefore, taking the relaxation time found after 250 sec, and applying it to the entire data set results in a curve that nearly represents the single element Maxwell model. However, as relaxation times from further into the experiment are used (500, 1000, 2000 sec), the curves begin to diminish, and do not reflect the Maxwell model. This means that the magnetic tape samples react in a much more viscoelastic fashion at the beginning of the experiment, and a much more elastic fashion as the experiment progresses. To account for the reduction in viscoelasticity, a multiple element Maxwell model could be implemented.

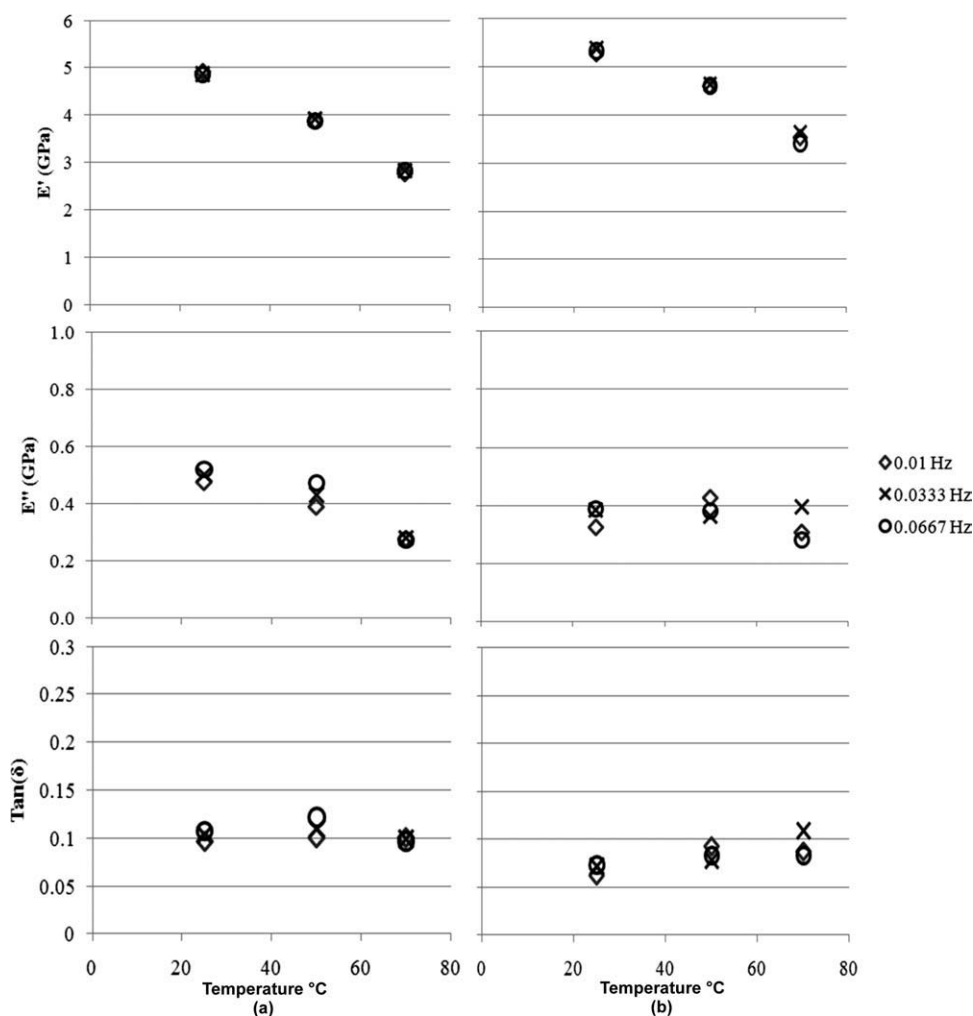


**Figure 16.** Storage modulus ( $E'$ ), loss modulus ( $E''$ ), and loss tangent [ $\text{Tan}(\delta)$ ] for (a) PEN substrate from tape and (b) PET substrate from tape. Data sets acquired using the ULDMA.

## SUMMARY AND CONCLUSIONS

### Conclusions

Thermal and mechanical properties of PEN, PET, M-PET, M-SPA tapes, as well as PEN and PET substrates, were measured and analyzed using ultra-low frequency dynamic mechanical analysis (ULDMA). The main difference between the PEN and PET molecular structures is the presence of a naphthalene ring in PEN, which is the primary reason the mechanical and thermal properties of these two magnetic tapes differ. The orientation of the naphthalene ring results in PEN having a more rigid structure than PET, making PEN more thermally stable, which is confirmed with a higher glass transition temperature. However, to increase the mechanical properties of PET, the samples undergo a tensilization process, which creates more ordered chains, and produces a stiffer, more elastic tape. This process is the reason the PET samples displayed a higher elastic and storage modulus in the frequency and temperature sweep ULDMA experiments than the PEN samples. The slope of the elastic and storage moduli of PEN,  $-0.0467 \text{ GPa}/^\circ\text{C}$  is greater (more negative) than that of PET,  $-0.0333 \text{ GPa}/^\circ\text{C}$ , because of the secondary movements associated with the naphthalene ring. This is

supported by the higher loss tangent values for PEN, which represent the energy dissipated during the cyclic loading and unloading. The PET samples, on the other hand, had a smaller slope for the moduli, proving that the tensilization process improved the elastic properties. However, the residual stresses present from the tensilization process eventually become relieved, near the glass transition temperature, which is lower than that of PEN. Once the glass transition temperature is reached, the slopes of the elastic and storage moduli begin to increase significantly, which is also represented by an increase in the loss tangent. The peak in the loss tangent, the  $\alpha$ -peak, signifies the location of the glass transition temperature. Additional ULDMA experiments at higher temperatures will more clearly show the glass transition temperatures for each of the samples. The PEN samples showed a larger phase angle and time delay than the PET samples, further evidence that PEN is more viscoelastic, while PET is more elastic.

Additionally, the relaxation times associated with PEN were lower than PET, suggesting that PEN can be modeled to more closely resemble a single element Maxwell viscoelastic model. These same trends were noticed for the PEN and PET substrates

**Table III.** Relaxation Times of Each Magnetic Tape Sample

	Frequency (Hz)	Temperature (°C)	$\tau$ (250) (s)	$\tau$ (500) (s)	$\tau$ (1000) (s)	$\tau$ (2000) (s)
PEN	0.0667	25	3,034	6,141	10,210	21,890
		50	2,007	3,000	5,127	11,060
		70	1,675	2,645	4,266	6,777
	0.0333	25	4,384	8,194	11,880	20,780
		50	2,319	3,237	5,980	11,650
		70	1,746	2,638	4,470	6,929
	0.01	25	10,600	20,920	34,160	76,460
		50	3,563	4,126	6,164	12,200
		70	2,035	3,294	5,882	11,590
PET	0.0667	25	12,080	18,090	37,090	379,800
		50	2,612	4,532	7,463	12,180
		70	1,705	2,129	3,358	7,274
	0.0333	25	5,754	9,929	21,380	35,160
		50	8,419	7,915	12,550	20,770
		70	3,199	5,431	6,342	8,254
	0.01	25	12,030	35,220	35,218	42,670
		50	11,240	8,690	11,440	21,120
		70	3,450	4,098	5,342	8,394
M-PET	0.0667	25	4,809	6,808	14,430	21,010
		50	4,501	6,155	8,457	15,210
		70	1,249	2,097	3,272	5,900
	0.0333	25	5,322	6,436	16,770	22,100
		50	5,717	6,699	9,950	16,150
		70	2,673	3,957	5,065	6,614
	0.01	25	6,828	12,090	33,780	58,950
		50	7,303	8,001	10,040	17,140
		70	8,090	4,899	6,682	10,360
M-SPA	0.0667	25	4,942	8,723	14,470	19,750
		50	2,534	4,052	6,272	13,040
		70	1,137	2,122	3,305	7,013
	0.0333	25	7,261	12,400	18,220	30,220
		50	3,604	4,516	6,660	13,369
		70	1,131	2,184	3,440	7,035
	0.01	25	7,402	12,990	18,370	33,640
		50	6,946	7,831	9,190	17,200
		70	4,569	6,475	7,839	11,380
PEN substrate from tape	0.0667	25	7,364	11,200	20,900	49,010
		50	2,821	4,329	6,064	16,380
		70	1,511	2,577	3,549	7,875
	0.0333	25	18,410	23,060	22,840	65,640
		50	5,663	7,624	11,580	19,130
		70	3,079	4,161	5,878	8,446
	0.01	25	11,240	17,730	35,020	43,020
		50	5,593	6,473	13,410	19,140
		70	4,521	5,194	6,260	11,620
PET substrate from tape	0.0667	25	17,370	27,670	75,540	146,800

TABLE III. Continued

	Frequency (Hz)	Temperature (°C)	$\tau$ (250) (s)	$\tau$ (500) (s)	$\tau$ (1000) (s)	$\tau$ (2000) (s)
		50	4,507	6,523	11,520	19,300
		70	1,076	1,765	3,959	7,790
	0.0333	25	13,810	15,544	64,270	130,700
		50	6,982	9,090	13,430	28,990
		70	1,266	1,865	4,328	7,932
	0.01	25	14,550	18,059	55,207	84,290
		50	7,430	9,359	16,770	29,530
		70	1,441	2,442	4,338	8,046

from tape, indicating that the properties found through ULDMA experiments are highly influenced by the substrate. However, the effect of the front and back coats of PEN and PET tapes did appear to decrease the dimensional stability of the tapes due to the fact that the PEN and PET substrates from tape demonstrated a higher elastic and storage modulus than their respective tapes with front and back coats. The bonds at the interface of the tape layers are weaker than those in the substrate, so the stress required to stretch the sample to the desired strain was less for the PEN and PET tapes. Also, the elastomeric binder used for the front coat could influence the viscoelastic behavior of the tape, although it is used to bind rigid magnetic particles together.

The M-PET and M-SPA samples showed very similar characteristics to each other in all of the analysis techniques. These samples demonstrated elastic and storage moduli similar to that of the PEN samples, including the presence of a slight initial relaxation. However, the slopes of these samples were the same as those for the PET samples,  $-0.0333$ , demonstrating the lesser extent to which temperature affects PET-based substrates. Neither of the samples showed the presence of the  $\beta^*$  peak in the loss modulus or loss tangent plots. The loss tangent plots for both samples did reveal a significant increase at 70°C, leading into the  $\alpha$ -peak. This  $\alpha$ -peak is occurring at lower temperatures than those in the PEN and PET plots, suggesting that the metalization process reduces the glass transition temperature, or makes the thermal properties more susceptible to changes at low frequencies.

These results demonstrate proof-of-concept for using dynamic mechanical analysis at ultra-low frequencies on magnetic tape samples. The custom ULDMA was utilized with actual tape and substrate samples. Fundamental molecular-level behavior was studied at these ultra-low frequencies or rates of strain application; and, in the limit as these frequencies reach a minimum, they approach the level of creep. Relaxation phenomena that lead to dimensional instabilities are influenced by the rate of strain application as well as temperature and humidity, and results from the ULDMA enable a fundamental understanding of the sources of these instabilities. Therefore, the well-developed science of DMA analysis has not only been used to understand the relaxation phenomena associated with molecular behavior, it can assist with the prediction of the archival life of

future tapes. This enables the design of future magnetic tapes that will be stored on a reel for 100+ years.

### Future Directions

This research has opened the door for additional research to be performed to gain an even better understanding of the effect of temperature and frequency on the mechanical and thermal properties of magnetic tapes. Additional ULDMA experiments need to be conducted at additional temperatures and frequencies to help with the critical evaluation of the ULDMA's capabilities including precision and range. As more data points are collected, the  $\alpha$ ,  $\beta$ , and  $\beta^*$  peaks will be identified more clearly. This will provide a better understanding of the molecular movements in the magnetic tapes at ultra-low frequencies, and how they affect the temperature at which the relaxation peaks occur. Also, additional ULDMA experiments should be performed on different combinations of tapes and substrates, such as front coat plus substrate, and back coat plus substrate. As previously discussed, tape substrates behave differently than their corresponding tapes with front and back coat. Therefore, these experiments will result in a better understanding of the effect each individual layer has on the dynamic stability of the tape. Additionally, further analysis on the ULDMA results can possibly be carried out using temperature-frequency superposition, a modified version of the time-temperature superposition

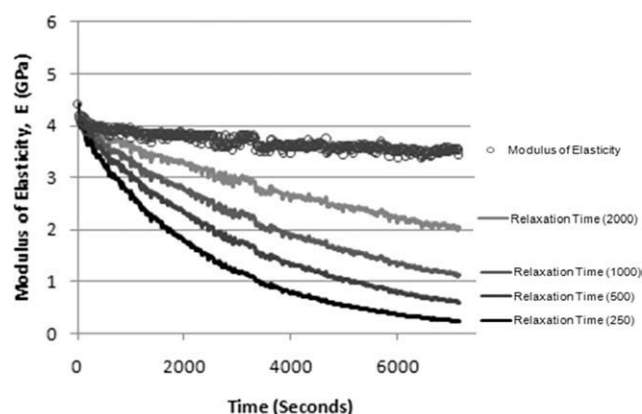


Figure 17. Curve fitting of ULDMA M-SPA data acquired at 0.0667 Hz and 50°C to Maxwell's relaxation curves for relaxation times of 250, 500, 1000, and 2000 sec.

analysis, which has been implemented for creep experiments.<sup>9,10,19</sup> This type of analysis could prove to be valuable because it would provide information regarding long-term archival magnetic tape characteristics.

#### ACKNOWLEDGMENTS

The authors thank the members of the Information Storage Industry Consortium (INSIC) Tape Program for their support and valuable input throughout the course of the research activity.

#### REFERENCES

1. International Magnetic Tape Storage Roadmap; Information Storage Industry Consortium: San Jose, CA, **2008**.
2. Bhushan, B. *Mechanics and Reliability of Flexible Magnetic Media*, 2nd ed.; Springer-Verlag: New York, **2000**.
3. Bhushan, B.; Ma, T.; Higashioji, T. *J. Appl. Polym. Sci.* **2002**, *83*, 2225.
4. Jefferies, C. Reference Guide—Hard Disk Drives. *Storage Review* May 16, **2007**.
5. Tonelli, A. *Polymer* **2002**, *43*, 637.
6. Ma, T.; Bhushan, B. *J. Appl. Polym. Sci.* **2003**, *89*, 548.
7. Ma, T.; Bhushan, B. *J. Appl. Polym. Sci.* **2003**, *89*, 3052.
8. Weick, B. *J. Appl. Polym. Sci.* **2011**, *120*, 226.
9. Weick, B. *J. Appl. Polym. Sci.* **2006**, *102*, 1106.
10. Weick, B. *J. Appl. Polym. Sci.* **2009**, *111*, 899.
11. Acton, K.; Weick, B. *J. Appl. Polym. Sci.* **2011**, *122*, 2884.
12. Cristea, M.; Ibanescu, S.; Cascaval, C.; Rosu, D. *High Performance Polym.* **2009**, *21*, 608.
13. Rummel, N. *Dynamic Mechanical Analysis of Magnetic Tapes at Ultra-Low Frequencies*. University of the Pacific, **2011**.
14. Weick, B. *Effects of Fiber Type on the Tribological Behavior of Polyamide Composites*. Virginia Polytechnic Institute and State University, **1993**.
15. Grassia, L.; D'Amore, A. *Phys. Rev. E.* **2006**, *74*, 021504.
16. Grassia, L.; D'Amore, A. *J. Polym. Sci. Part B: Polym. Phys.* **2009**, *47*, 724.
17. Bhushan, B.; Tao, Z. *J. Appl. Polym. Sci.* **2004**, *92*, 1319.
18. Bendat, J.; Piersol, A. *Random Data: Analysis and Measurement Procedures*; Wiley: New York, **1986**.
19. Higashioji, T.; Bhushan, B. *J. Appl. Polym. Sci.* **2002**, *84*, 1477.
20. Canadas, J.; Diego, J.; Sellares, J.; Mudarra, M.; Belana, J.; Diaz-Calleja, R.; Sanchis, M. *Polymer* **2000**, *41*, 2899.